

AD-A238 879



2

OFFICE OF NAVAL RESEARCH
Contract N00014-91-J-1045
R&T Code 4132047---02-1

TECHNICAL REPORT NO. 5

Blends of Crystallizable Polybutadiene Isomers:
Compatibilization by Addition of Amorphous Diblock Copolymer

by

Moira Marx Nir and Robert E. Cohen
Department of Chemical Engineering
Massachusetts Institute of Technology
Cambridge, MA 02139-4307

July 24, 1991

DTIC
ELECTE
JUL 29 1991
S B D

Reproduction in whole or in part is permitted for any purpose of the U.S. government.

This document has been approved for public release and sale; its distribution is unlimited.

91-06399



91 7 29 101

REPORT DOCUMENTATION PAGE

1a. REPORT SECURITY CLASSIFICATION		1b. RESTRICTIVE MARKINGS	
2a. SECURITY CLASSIFICATION AUTHORITY		3. DISTRIBUTION / AVAILABILITY OF REPORT	
2b. DECLASSIFICATION / DOWNGRADING SCHEDULE		approved for public release; distribution unlimited	
4. PERFORMING ORGANIZATION REPORT NUMBER(S) Technical Report No. 5		5. MONITORING ORGANIZATION REPORT NUMBER(S)	
5a. NAME OF PERFORMING ORGANIZATION MIT, Building 66, Room 554	6a. OFFICE SYMBOL (If applicable)	7a. NAME OF MONITORING ORGANIZATION Office of Naval Research	
5c. ADDRESS (City, State, and ZIP Code) MIT, Building 66, Room 554 Cambridge, MA 02139-4307		7b. ADDRESS (City, State, and ZIP Code) 800 N. Quincy Street Arlington, VA 22217	
8a. NAME OF FUNDING / SPONSORING ORGANIZATION ONR	8b. OFFICE SYMBOL (If applicable)	9. PROCUREMENT INSTRUMENT IDENTIFICATION NUMBER N00014-91-J-1045	
8c. ADDRESS (City, State, and ZIP Code) 800 N. Quincy Street Arlington, VA 22217		10. SOURCE OF FUNDING NUMBERS	
		PROGRAM ELEMENT NO.	PROJECT NO. 4132047
		TASK NO. 02	WORK UNIT ACCESSION NO. 1
11. TITLE (Include Security Classification) Blends of Crystallizable Polybutadiene Isomers: Compatibilization by Addition of Amorphous Diblock Copolymer			
12. PERSONAL AUTHOR(S) Moira Marx Nir and Robert E. Cohen			
13a. TYPE OF REPORT Technical Report	13b. TIME COVERED FROM _____ TO _____	14. DATE OF REPORT (Year, Month, Day) July 24, 1991	15. PAGE COUNT 47
16. SUPPLEMENTARY NOTATION Edited condensation of doctoral thesis.			
17. COSATI CODES		18. SUBJECT TERMS (Continue on reverse if necessary and identify by block number)	
FIELD	GROUP	semicrystalline polymer blends	
	SUB-GROUP	compatibilization of polymer blends	
19. ABSTRACT (Continue on reverse if necessary and identify by block number) Precipitated blends of two crystallizable polybutadiene (PBD) isomers were characterized in terms of crystallization and phase behavior, morphology, and tensile mechanical properties. The isomers are syndiotactic 1,2 PBD ($M_v=32.5k$ g/mol) and trans 1,4 PBD ($M_v= 425k$ g/mol). As predicted by Flory-Huggins theory, the blends exhibit heterogeneous behavior over the full range of composition. Degree of heterogeneity due to precipitation is on the order of 5 μ or less, whereas spincast blends of amorphous (atactic 1,2 PBD/mixed cis+trans 1,4 PBD) homopolymers give macrodomains up to 50 μ in diameter. Tensile properties of the crystalline blends are intermediate between those of the corresponding crystalline homopolymers, while tensile properties of the amorphous blends are generally worse than either of the amorphous homopolymers. But in both cases, property enhancement is evident at approximately 10% 1,2 PBD content. Additionally, mechanical properties at break of the s-1,2 PBD/trans 1,4 PBD crystalline blends are improved by addition of 5-10% amorphous 1,2 PBD/1,4 PBD diblock copolymer. (continued on back)			
20. DISTRIBUTION / AVAILABILITY OF ABSTRACT <input checked="" type="checkbox"/> UNCLASSIFIED/UNLIMITED <input type="checkbox"/> SAME AS RPT. <input type="checkbox"/> DTIC USERS		21. ABSTRACT SECURITY CLASSIFICATION	
22a. NAME OF RESPONSIBLE INDIVIDUAL		22b. TELEPHONE (Include Area Code)	22c. OFFICE SYMBOL

The effect of block molecular weight and micro-phase behavior on compatibilization of the crystalline homopolymers was also investigated. Heterogeneous diblocks enhance blend properties to a greater extent than homogeneous diblocks. In blends with enhanced properties, percent coverage of interfacial surface area by diblock is on the order of 10%.



Accession For	
NTIS GRA&I	<input checked="" type="checkbox"/>
DTIC TAB	<input type="checkbox"/>
Unannounced	<input type="checkbox"/>
Justification	
By _____	
Distribution/ _____	
Availability Codes	
Avail and/or	
Dist	Special
A-1	

I. Introduction

IA. Background

Most binary homopolymer blends are thermodynamically immiscible. In immiscible blends, non-equilibrium islands or macrodomains of one polymer form in a matrix of the other and interfacial adhesion between the phases is usually poor. As a result, properties of incompatible blends are often much poorer than those of either homopolymer.

But under appropriate conditions, blends of immiscible homopolymers X and Y can be compatibilized by the corresponding XY diblock copolymer. Copolymer can reduce the domain size of the dispersed phases, decrease interfacial tension, and enhance adhesion across the homopolymer phase boundaries. The altered morphology leads to improved properties (Roe and Rigby, 1987). Extent of dispersion and reinforcement is dependent on the molecular weights (MWs) of the blocks relative to the corresponding homopolymer MWs, and on the percent and nature of the diblock present in the blend.

At high diblock concentrations when the homopolymer MWs are not greater than the corresponding block MWs, the homopolymers may be solubilized in the microdomains of the like components of the copolymer (Reiss et al., 1967; Kohler et al., 1968; Inoue et al., 1970; Tanaka et al., 1991). In this case, homogeneous (single-phase) diblocks tend to have better compatibilizing potential than do heterogeneous (micro-phase separated) diblocks (Ramos and Cohen, 1977). Diblocks of equal segment lengths are the most efficient emulsifying agents, and if the MWs of the two blocks are unequal, the homopolymer corresponding to the larger block is preferentially solubilized into the diblock copolymer.

At low concentrations of diblock and if the block MWs are not greater than the corresponding homopolymer MWs, the diblocks locate preferentially at the homopolymer interfaces and are solubilized in the homopolymer domains. Micro-phase separation of the blocks promotes localization at the interface (Kryszewski, 1980) and extension into homopolymer domains, perhaps making compatibilization dependent on the MW of the longer copolymer block (Shull and Kramer, 1990). Recent work by Elamans et al. (1990) showed that with less than 1% diblock, the interfacial tension was significantly lowered in such blends. These results seem to be applicable not only for systems of amorphous homopolymers and diblocks, but also for

systems with crystallizable polymer components (Drzewinski, 1986; del Giudice et al., 1985).

Creton et al. (1991) propose that interfacial reinforcement occurs only when the blocks entangle with both homopolymers. Therefore, the shorter block must not be shorter than the average chain length between entanglements of the homopolymers. If the MW is less the critical minimum, the copolymer will still act as a surfactant to decrease interfacial tension and modify morphology, but it will not prevent failure at the interface when high tensile stress is applied.

Otherwise, when the conditions for solubilization of diblock into homopolymer or homopolymer into diblock are not met, the diblocks and homopolymers segregate from each other to form independent phases.

Thermodynamic models have been developed by Xie et al. (1986, 1988) and Meier (1977) for solubilization of homopolymer into diblock domains, and by Noolandi et al. (Whitmore and Noolandi, 1985; Noolandi and Hong, 1984) and Leibler (Leibler, et al., 1983; Roe, 1986; Leibler, 1988) for solubilization of blocks into homopolymer domains. Noolandi's and Leibler/Roe's work predict a critical diblock concentration above which diblocks form micelles rather than mix with homopolymers. Up to this concentration, the theories predict the observed lowering of interfacial tension in blends with two immiscible homopolymers (Noolandi and Hong, 1984; Leibler, 1988). The Leibler/Roe model was found to be qualitatively correct in Kinning et al.'s (1991) experimental work with polystyrene/polybutadiene ternary systems, but it predicted critic micelle concentrations at least 1 order of magnitude too high.

Del Giudice et al. (1985) emulsified blends of isotactic polypropylene and isotactic polystyrene by addition of (isotactic polypropylene)/(isotactic polystyrene) diblock copolymer. In this case, both homopolymers and both blocks of the diblock copolymer were crystalline. The diblock was synthesized via sequential Zeigler-Natta (ZN) polymerization. However, ZN catalysis is difficult because it gives polymers with short lifetimes, thus sequential ZN polymerization is even more difficult (Willis, 1984). In fact, outside of the diblock in del Giudice's work, sequential ZN polymerization is virtually undocumented. Thus the ability to create diblocks in which both blocks are crystalline is severely limited at this time.

As an alternative to emulsifying two crystallizable homopolymers with the matching crystalline diblock copolymer, we considered adding amorphous

diblock to crystallizable homopolymer blends, where the blocks correspond to amorphous isomers of the homopolymers. No similar investigation was found in the literature. Compared to synthesizing copolymers with two crystalline blocks, synthesizing amorphous diblocks is relatively easy via anionic-to-anionic transformations or coupling of blocks previously synthesized. If crystalline homopolymer blends can be compatibilized by amorphous diblocks, the commercial implications are much greater than if these blends can only be compatibilized by crystalline diblocks.

The reason why this approach is feasible is that all crystalline polymers contain an amorphous fraction that is unable to crystallize. Crystallinity contents of only 40%-50% can constitute highly crystalline materials. In solution or in a melt, the crystallizable portions become amorphous, thus polymer chains from two materials that differ only in tacticity or cis/trans structure become less distinguishable from each other and are able to thermodynamically mix. For example, polymer blocks with a given atactic structure may mix with homopolymer that is syndiotactic or isotactic but otherwise structurally identical to the atactic blocks; and similarly, blocks with a mixed cis+trans structure are expected to mix with homopolymer that is primarily all-cis or all-trans but otherwise structurally identical to the cis+trans block. Then, upon subsequent crystallization, the amorphous blocks may remain thermodynamically mixed with amorphous homopolymer regions and thereby compatibilize the homopolymers.

(The concept of tacticity is illustrated in Figure 1. In isotactic polymers, a given monomer side group is always aligned on the same side of the polymer backbone, and in syndiotactic polymers, the pendant group alternates from side-to-side along the backbone. The inherent stereo-regularity in polymers synthesized via isotactic or syndiotactic 1,2 addition or via cis or trans 1,4 addition of alpha-olephin and diene monomers allows them to crystallize, as long as they do not contain overly bulky side groups (Billmeyer, 1984). In atactic polymers, the pendant group is aligned in a random manner, thus the polymers are not stereo-regular and typically do not crystallize.)

IB. Project Goals

In light of the discussion above, the objectives of our research program were as follows:

- 1) Characterize binary blends of crystallizable syndiotactic 1,2 PBD and trans 1,4 polybutadienes (PBD) in terms of crystallization and phase behavior, morphology, and mechanical properties.
- 2) Investigate the effects of amorphous (atactic 1,2 PBD)/(mixed cis+trans 1,4 PBD) diblocks on the above-mentioned properties in blends of syndiotactic 1,2 PBD and trans 1,4 PBD homopolymers.

The second goal initially involved determining whether or not amorphous diblock copolymer played any role at all in such a system. Then we analyzed effects of diblock content, block MWs, and phase-behavior of the added diblocks.

The monomeric units for 1,2 PBD and 1,4 PBD are given in Figure 2, and the chain conformations of the four stereoisomers of PBD - trans 1,4 PBD, cis 1,4 PBD, syndiotactic 1,2 (s-1,2) PBD and isotactic 1,2 PBD - are shown in Figure 3.

II. Experimental Section

Both homopolymers and all diblock copolymers in this work were provided by Dr. Adel Halasa (Goodyear Tire and Rubber Company, Akron, OH).

We used three amorphous (atactic 1,2 PBD)/(mixed cis+trans 1,4 PBD) diblock copolymers. Two of the three diblocks were reported by Cohen and Wilfong (1982) as having block molecular weights of 30k/50k g/mol (1,2/1,4 PBD) and 30k/200k g/mol. The 30k/50k diblock is heterogeneous and the 30k/200k diblock is homogeneous at 25°C. The third diblock has block molecular weights of 60k/120k and is heterogeneous at 25°C. As determined from ¹H NMR, the 1,4 PBD blocks are approximately 90% 1,4 PBD and the 1,2 PBD blocks are approximately 95%-99% or more 1,2 PBD.

Blends were prepared in batches of 1.00±0.02g polymer in tetralin (1,2,3,4 tetrahydronaphthalene). Solution concentration was 2% polymer and 0.02% Irganox 1076 antioxidant. The polymer components were added to preheated tetralin at 135±3°C and then stirred at this temperature for exactly 60 minutes. The hot blend solution was then drip precipitated into stirred, cold MeOH. The ratio of MeOH to tetralin was at least 6:1. Next, the precipitated

polymer was vacuum filtered and dried at room temperature in a vacuum oven or hood until it achieved constant weight. To make films, the precipitated powders were compression-molded in the melt (200°-205°C) for 2 minutes on a preheated Carver table-top press. The mold was immediately placed between slabs of dry ice to achieve rapid cooling. Resulting film thickness was 0.3-0.7 mm.

Forty-nine different compositions were prepared by this method, comprising binary homopolymer blends and blends of homopolymers plus one of the three diblock copolymers. All of the compositions are depicted in Figure 4.

Differential scanning calorimetry tests (Perkin-Elmer DSC-4) were performed in a nitrogen atmosphere at a heating rate of 20°C/min and a quench-cooling rate of 320°C/min. Error associated with DSC operation is approximately $\pm 2^\circ\text{C}$ for temperature data and ± 1 cal/g for enthalpy data, as determined from duplicate trials.

Dynamic mechanical properties of 40mm x 3mm x 0.3-0.7mm films were obtained via a Rheovibron Direct Reading Dynamic Viscoelastometer (Model DDV-II-C, Toyo Baldwin Co., Ltd., Tokyo, Japan) operated at 11 Hz. Samples were heated at a rate of 2°-4°C/min in a nitrogen atmosphere. Error associated with analysis of temperature is about $\pm 5^\circ\text{C}$.

Microscopy tools included a Nikon AFX-II Optiphot-pol Polarizing Microscope fitted with a Polaroid 4x5 Land film attachment and Mettler FP82 Hot Stage, a Cambridge (England) S240 Scanning Electron Microscope (SEM) operated at 1.0 kV and 15 kV, and a Phillips 300 Transmission Electron Microscope (TEM) operated at 100 keV. SEM samples were lightly gold-coated. TEM samples were sulfur stained for 4-24 hours by the method of Smith and Andries (1974) and then microtomed to thicknesses of 700Å-1300Å.

X-ray scattering patterns (Rigaku X-ray Diffraction System) were detected via a rotating anode x-ray generator and point focus for both wide angle and small angle equipment (WAXS, SAXS). The $\text{CuK}\alpha$ x-ray source emits radiation with a wavelength of 1.54Å.

Room temperature tensile properties were obtained on a Model 4201 Instron device (Instron Corporation, Canton, MA). Sections of compression-molded films were cut into "micro-dogbone" specimens with test dimensions of approximately 5.2 mm x 2 mm x 0.3-0.7 mm. Typically, three specimens were tested per blend sample. For the most rubbery materials, only two specimens

were tested if they gave nearly identical results. Crosshead speed was 0.2 mm/min.

III. Homopolymer Characterization

IR data for our homopolymers match literature spectra reported by Morero et al. (1960, 1962) for s-1,2 PBD and trans 1,4 PBD. From ^1H NMR, we calculated that our s-1,2 PBD has approximately $95\pm 3\%$ 1,2 PBD content and that our trans 1,4 PBD has approximately $91\pm 6\%$ 1,4 PBD content. No cis 1,4 PBD peaks were discernable in either ^1H or ^{13}C NMR spectra for the trans 1,4 PBD homopolymer. A single ^{13}C NMR peak at 114.4 ppm, as opposed to a triplet, indicates that the s-1,2 PBD homopolymer contains negligible amounts of isotactic and atactic segments.

WAXS scans of our s-1,2 PBD material gave peaks at 2θ values of 13.4° , 16.1° , 21.1° , 23.4° . Via Bragg's Law,

$$d = \lambda / (2 \sin \theta),$$

the peaks correspond to d-spacings of 6.6\AA , 5.5\AA , 4.2\AA , and 3.8\AA . These peaks were also observed by Natta and Corradini (1956). Our trans 1,4 PBD material exhibited a single peak at a 2θ value of 22.4° , which corresponds to a d-spacing of 4.0\AA . Again, our data agree with data in the literature by a number of researchers (Bermudez and Fatou, 1972; Iwayanagi et al., 1968; Natta et al., 1962). Scans of each of these samples are shown in Figure 5.

Homopolymer molecular weights were determined by viscometry. After samples are mixed for one hour in tetralin at 135°C , s-1,2 PBD viscometry molecular weight (M_v) is approximately 32.5k g/mol and trans 1,4 PBD M_v is approximately 425k g/mol. Degree of polymerization, x , is thus 601 ± 59 for s-1,2 PBD and 7857 ± 277 for trans 1,4 PBD.

Rheovibron data gave glass transition (T_g) onsets and peaks for trans 1,4 PBD at -80°C to -85°C and -51°C to -43°C , respectively, and T_g onsets and peaks for s-1,2 PBD at 5°C to 35°C and 44°C to 54°C . There was no significant difference in glass transition data for unprecipitated (as-received) and precipitated materials. On the other hand, melting points ranged from 186°C to 194°C for s-1,2 PBD and 132°C to 150°C for trans 1,4 PBD, depending on thermal history. Table 1 lists DSC-determined homopolymer melting points and percent crystallinities as a function of thermal history. Melting of as-received powders substantially lowers their crystallinity but has less of an effect on the resulting melting points than do other thermal treatments. Conversely, upon

precipitating homopolymers from solution, the total amount of crystallinity is nearly retained yet the melting points are significantly lowered. Thus the crystallites that form during precipitation are probably smaller and less perfect than the original unprecipitated crystallites.

For precipitated, compression-molded homopolymers that were otherwise not subjected to elevated temperatures, *s*-1,2 PBD melting point (T_s) is 186°C, *trans* 1,4 PBD melting point (T_t) is 137°C, percent crystallinity of *s*-1,2 PBD ($\%C_s$) is 36%, and percent crystallinity of *trans* 1,4 PBD ($\%C_t$) is 52%. Table 2 summarizes characterization data for precipitated, compression-molded homopolymers.

As for the kinetics of crystallization, crystallization half-times, $\tau_{1/2}$, are plotted as a function of undercooling in Figure 6. At undercoolings of 16.5°C for *trans* 1,4 PBD and 30.3°C for *s*-1,2 PBD, crystallization half-times are less than 50 seconds. With these relatively fast crystallization properties, it is not possible to "lock-in" melt morphology of either homopolymer by transferring melt samples directly into liquid nitrogen. Also, the fast crystallization kinetics may have masked any difference in melting points and crystallinity contents for samples isothermally crystallized at various temperatures below their melting points.

Polarized light microscopy showed *s*-1,2 PBD spherulites approximately 12 μ in diameter when crystallized at 18.5°C undercooling for 8 minutes. *Trans* 1,4 PBD crystallized into rod-like structures 5 μ to 10 μ in length when held at an undercooling of 11.5°C for 8 minutes. In sulfur-stained TEM specimens, we observed regularly spaced segments approximately 200Å apart in *s*-1,2 PBD samples. In stained *trans* 1,4 PBD, segments about 1000Å were apparent but were spaced less evenly than in the *s*-1,2 PBD specimens.

Stress-strain data from Instron tensile tests on precipitated homopolymers are given in Figure 7. *S*-1,2 PBD has a modulus that is more than twice that of *trans* 1,4 PBD, but it breaks at much lower elongations. At higher strains, *trans* 1,4 PBD displays rubbery behavior. These results are sensible considering that at the test temperature of 25°C, *s*-1,2 PBD is at or slightly below its glass transition while *trans* 1,4 PBD is at least 100°C above its T_g .

IV. Homopolymer Binary Blends

IVA. Melt Model

A Flory-Huggins model can be applied to obtain phase diagrams of binary blends of amorphous polymers at constant pressure. This theory predicts upper critical solution temperatures (UCST) but does not predict experimentally observed lower critical solution temperatures. However, it is sufficient and appropriate for blends of non-polar, non-interacting polymer pairs (deGennes, 1979), such as polybutadienes. With this model,

$$\Delta G_{\text{mix}}/V = \Delta H_{\text{mix}}/V - T\Delta S_{\text{mix}}/V = B\phi_1\phi_2 + RT[(\phi_1/v_1)\ln\phi_1 + (\phi_2/v_2)\ln\phi_2]$$

where ΔG_{mix} is the free energy of mixing, ΔH_{mix} is the enthalpy of mixing, T is temperature, and ΔS_{mix} is the entropy of mixing; V is total volume, ϕ_1 and ϕ_2 are the volume fractions of polymers 1 and 2, v_1 and v_2 are the molar volumes, R is the gas constant, and B is the polymer-polymer interaction parameter (Paul, 1985). B is equal to $(\delta_1 - \delta_2)^2$ in Scatchard-Hildebrand notation (Hildebrand and Scott, 1964), $\chi RT/v_1$ in Flory's notation (Flory, 1953) and $\chi x/v_1$ in most other χ notations (Paul, 1985), with x equal to degree of polymerization.

Note that

$$\phi_i = N_i v_i / V$$

where i corresponds to component 1 or 2 and N is the number of moles of polymer chains. In terms of total volume, the extensive free energy of mixing can be written

$$\Delta G_{\text{mix}} = G_{\text{mix}} - G^\circ_{\text{mix}} = B\phi_1 N_2 v_2 + RT[N_1 \ln\phi_1 + N_2 \ln\phi_2] = B\phi_2 N_1 v_1 + RT[N_1 \ln\phi_1 + N_2 \ln\phi_2]$$

The chemical potentials, μ_1 and μ_2 , are defined as $\partial G_{\text{mix}}/\partial N_1$ and $\partial G_{\text{mix}}/\partial N_2$, respectively, and are equal to $\partial \Delta G_{\text{mix}}/\partial N_1$ and $\partial \Delta G_{\text{mix}}/\partial N_2$ since G°_{mix} is a constant. Thus, in terms of ϕ_2 ,

$$\mu_1 = Bv_1\phi_2^2 + RT[\phi_2(1-v_1/v_2) + \ln(1-\phi_2)]$$

$$\mu_2 = Bv_2(1-\phi_2)^2 + RT[(1-\phi_2)(1-v_2/v_1) + \ln(\phi_2)]$$

In order for blends to be homogeneous, the free energy of mixing must be negative. Then, the binodal curve depicts the compositions of coexisting equilibrium phases as a function of temperature, assuming nucleation is not suppressed so as to prevent phase separation. Below the binodal curve in an UCST system, two equilibrium phases are present (A, B), i.e. the system is "heterogeneous". Above it, no phase separation occurs, i.e. the system is

"homogeneous." For a given temperature, the two points on the binodal curve simultaneously satisfy the following two conditions:

$$\mu_1(\phi_2^A) = \mu_1(\phi_2^B) \quad \text{and} \quad \mu_2(\phi_2^A) = \mu_2(\phi_2^B)$$

The spinodal curve and critical point are defined, respectively, by

$$\begin{aligned} \partial^2 \Delta G_{\text{mix}} / \partial N_1^2 &= 0, \\ \text{and } \partial^3 \Delta G_{\text{mix}} / \partial N_2^3 &= 0. \end{aligned}$$

The latter expression leads to

$$\phi_{2\text{crit}} = v_1^{1/2} / (v_2^{1/2} + v_1^{1/2}).$$

We applied this model for mixtures of amorphous 1,2 PBD and 1,4 PBD materials in order to predict the phase behavior of s-1,2 PBD/trans 1,4 PBD blends in the melt state. Phase diagrams were developed for blends of 1,2 PBD with molecular weight 32.5k g/mol and 1,4 PBD molecular weight of 425k g/mol, since these molecular weights correspond to the average M_v values of our homopolymers. Values for v_1 , v_2 , and B were calculated from group contribution parameters (Van Krevelen, 1976), assuming $B = (\delta_1 - \delta_2)^2$. The binodal and spinodal curves are shown in Figure 8.

These phase diagrams predict that 1,2 PBD/1,4 PBD binary blends with MWs of 32.5k g/mol and 425k g/mol, respectively, are heterogeneous at temperatures less than the PBD degradation temperature (220°C) nearly all of the composition spectrum. The region that corresponds to a melt of our s-1,2 PBD and trans 1,4 PBD blends falls above the s-1,2 PBD melting point around 460K (187°C). The model therefore predicts that our s-1,2 PBD/trans 1,4 PBD system is heterogeneous in the melt at any temperature and composition of practical interest.

IVB. Background: Possibilities for Binary Blends of Crystalline Homopolymers

Homogeneous mixing of one crystallizable polymer and one amorphous polymer leads to classical melting point depression of the crystalline component, as predicted by Scott (1949) and Flory (1953) (Nishi and Wang, 1975; Rim and Runt, 1984; Chow, 1990). Burghardt (1989) extended Flory's expressions to blends of two crystallizable polymers and calculated phase diagrams for various interaction parameters.

Heterogeneous blends of two crystallizable polymers give two distinct melting points for any composition, i.e. one melting point per homopolymer. Burghardt's analysis predicts only negligible melting point depression for each component over the total composition range in such a system.

On the other hand, homogeneous blends of two crystallizable polymers may form eutectic or isomorphous systems, which are characterized by a single melting point for any composition. No cases of true polymer-polymer eutectics are documented (Manson and Sperling, 1976; Nishi et al., 1988), but eutectic solidification has been observed for a few polymer/monomer blends (Smith and Pennings, 1974; Wittmann and St. John Manley, 1977; Hodge et al., 1982; Suzuki et al., 1984; Tanaka et al., 1984). Isomorphous cocrystallization is rare but has been observed (Natta et al., 1969, Paul and Newman, 1978; Olabisi et al., 1979; Tanaka et al., 1990).

A final possibility for two crystallizable homopolymers that are homogeneous in a melt is that they may crystallize independently while the fractions that ultimately remain uncrystallized still mix homogeneously (Escala and Stein, 1979). The amorphous material can then reside between crystalline lamellae and/or be accepted in spherulitic or other crystalline structures (Russell et al., 1988).

As with amorphous polymer blends, thermodynamics of crystalline systems must be considered in conjunction with non-equilibrium effects. Polymer diffusion plays a role in determining morphology. In addition, crystallization kinetics and the interplay between crystallization and phase behavior affect blend morphology (Chow, 1990). By altering a crystallizable blend's thermal and processing history, we can obtain quite varied morphologies for a given blend composition (Runt and Rim, 1982; Tanaka and Nishi, 1985).

IVC. Characterization of Crystallizable PBD System

Room temperature WAXS 2θ scans give distinct peaks for both components in binary blends of s-1,2 PBD and trans 1,4 PBD, as shown in Figure 9 for a 50/50 blend. DSC and light microscopy studies reveal two distinct melting points in every binary blend, i.e. one melting point per component. These results indicate that blends of s-1,2 PBD and trans 1,4 PBDs do not yield isomorphous or eutectic structures.

Plots of $\tan \delta$ versus temperature give two recurring transitions in every blend sample. One of the transitions corresponds to the T_g of the trans 1,4 PBD component between -88°C and -43°C , the other transition corresponds to the T_g of the s-1,2 PBD component between 5°C and 62°C . The presence of one T_g per component signifies that the blends are heterogeneous at and below

the T_g of s-1,2 PBD. In blends with a trans 1,4 PBD content greater than 66%, we observed an additional transition between -100° and -81°C that corresponds to the T_g of cis 1,4 PBD or mixed cis+trans 1,4 PBD.

X-ray scattering studies imply that our binary blends are also heterogeneous in the melt. Amorphous halos of the melted blends comprise both amorphous peaks of trans 1,4 PBD and s-1,2 PBD homopolymer in the melt. Intensity plots in Figure 10 for the homopolymers and a 67/33 blend illustrate this point. These results verify the prediction of our thermodynamic model in Section IVA.

Blend melting points are slightly depressed from homopolymer values, as shown in Figure 11 as a function of trans 1,4 PBD content and as predicted by Burghardt (1989) for immiscible crystalline binary polymer systems. Trans 1,4 PBD crystallization is influenced more adversely by the presence of the s-1,2 PBD component than vice-versa. For instance, blends with 5-10% trans 1,4 PBD gave T_t values that were 8° - 11°C lower than homopolymer T_t values whereas blends with 5-10% s-1,2 PBD gave T_s values only 2° - 3°C lower than homopolymer T_s values. Similarly, $\%C_t$ falls significantly as s-1,2 PBD is added to trans 1,4 PBD, but $\%C_s$ does not drop as trans 1,4 PBD is added s-1,2 PBD, as depicted in Figure 12. Already-crystallized s-1,2 PBD chains may act as rigid barriers during subsequent crystallization of the trans 1,4 PBD component.

Light micrographs of a precipitated, compression-molded 75/25 (s-1,2 PBD/trans 1,4 PBD) blend at 140°C reveal s-1,2 PBD spherulites about 1μ to 5μ in diameter surrounded by melted domains of trans 1,4 PBD about 1μ to 5μ in diameter. In TEM micrographs of 67/33, 50/50, and 33/67 blends, we observed the same 1000\AA -spaced segments found in micrographs of trans 1,4 PBD homopolymer. The quantity of segments correlates with the amount of trans 1,4 PBD present. In 50/50 and 33/67 blends, we also distinguished the smaller 200\AA -spaced segments characteristic of s-1,2 PBD homopolymer. Based on micrographs from all of these blends, s-1,2 PBD domains are on the order of 0.2μ to 2μ when s-1,2 PBD constitutes less than 50% of the blend, and trans 1,4 PBD domains are between 0.5μ and 5μ when trans 1,4 PBD constitutes less than 50% of the blend.

Wilfong (1981) studied heterogeneous binary blends of amorphous 1,2 PBD ($M_w=90\text{k g/mol}$) and 1,4 PBD ($M_w=100\text{k g/mol}$). The blend compositions were 12/88 (1,2 PBD/1,4 PBD) and 38/62 and they contained 1μ - 50μ spherical macrodomains of 1,2 PBD in a matrix of 1,4 PBD. Macrodomains in the

crystalline PBD blends we prepared by precipitation were not greater than 5μ - 10μ in size, as evidenced from the light micrographs presented earlier. In general, finer degrees of heterogeneity can be achieved through precipitation than through spincasting because precipitation is a quick process that does not allow for gross phase separation.

In Wilfong's blends, the moduli and mechanical properties at break are well below the weighted average of the corresponding homopolymer properties, as expected of most incompatible systems. The exception is percent elongation at break of the 12/88 blend, which has a value greater than that of either amorphous homopolymer. Tensile properties of crystalline blends of s-1,2 PBD and trans 1,4 PBD show the following trends: Modulus and yield stress decrease while stress and percent elongation at break increase as a function of increased trans 1,4 PBD content. Plots of these properties as a function of trans 1,4 PBD content are given in Figure 13. Mechanical properties at break exhibit a maximum with the 10/90 blend, otherwise blend data all fall between the homopolymer property values and are close to the weighted average of the corresponding homopolymer properties. The fact that our heterogeneous crystalline blends do not have mechanical properties inferior to those of the homopolymers is likely due to the relatively fine dispersion of phases achieved through precipitation.

On the other hand, mechanical integrity of some of the 33/67, 50/50, and 67/33 specimens was poorer than that of the homopolymers. These specimens split along the axis of tension prior to breaking at the axis perpendicular to the applied tension. Such behavior is characteristic of oriented polymers in heterogeneous mixtures, thus the tensile testing process may have imposed orientation in at least one of the components.

Finally, property enhancement in Wilfong's 12/88 amorphous PBD blend and in our 10/90 crystalline PBD blend suggests that the 1,2 PBD component acts as a reinforcing filler at these concentrations. This phenomenon deserves further investigation.

V. Blends with Amorphous Diblock Copolymer: Characterization and Discussion

VA. Effects of Adding Amorphous Diblock Copolymer

A number of significant effects result when diblock copolymer is added to blends of s-1,2 PBD and trans 1,4 PBD. First, all compositions that we studied

are heterogeneous at room temperature, as determined by the presence of at least two glass transitions. One transition corresponds to 1,2 PBD and the second corresponds to 1,4 PBD. The only exception may be blends of 30k/200k diblock plus trans 1,4 PBD homopolymer.

Second, when the content of diblock is low, specifically $\leq 10\%$, some specimens still fractured along the axis of tension during Instron tensile testing. The compositions of these specimens are circled in Figure 14. Note that they all have trans 1,4 PBD/s-1,2 PBD (t/s) ratios less than 1.0. The fact that ternary blends with higher diblock contents did not fracture in this manner is understandable if the additional rubber content reduced interfacial stresses between domains of trans 1,4 PBD and s-1,2 PBD, and thus prevented the heterogeneous crystalline regions from violently separating and propagating such a fracture.

Third, mechanical properties were significantly altered by addition of small amounts of diblock. Tensile modulus and yield stress dropped sharply in blends with only 5% diblock content, and stress and percent elongation at break peaked in value at low concentrations of diblock when trans 1,4 PBD was also present. These properties are plotted as a function of diblock content in Figures 15-18. Also, in $t/s=1/2$ blends with low diblock content, percent-crystallinity of the trans 1,4 PBD component deviated slightly from the norm. Percent-crystallinity of the s-1,2 PBD component, on the other hand, was relatively constant in all samples. All of these results are not simply due to the presence of small amounts of any rubber since the phase behavior of the added diblock affected the degree of the observed phenomena, as is discussed in Section VB.

Fourth, there is some sort of interaction between the diblocks and trans 1,4 PBD that does not also occur between the diblocks and s-1,2 PBD. Glass transition peaks and onsets for both the 1,2 PBD and 1,4 PBD components were relatively constant in all blends, except when diblock was added to trans 1,4 PBD alone. In the latter case, T_g peak values for 1,4 PBD were dependent on sample composition. Figure 19 shows $\tan \delta$ curves for blends of diblock with trans 1,4 PBD, ranging from pure diblock at the top to pure trans 1,4 PBD at the bottom. In addition, for the case of component crystallinities in $t/s=1/2$ blends, the trans 1,4 PBD component but not the s-1,2 PBD component was slightly altered by the presence of diblock in small amounts, as described in the previous paragraph. Also, stress and percent elongation at break peaked in

blends with low diblock content, as discussed above, but only when the blends contained trans 1,4 PBD as well. Finally, interaction between the diblocks and trans 1,4 PBD may explain why ternary blends with more trans 1,4 PBD than s-1,2 PBD never fractured along the axis of tension, even with very low diblock contents.

VB. Addition of Heterogeneous versus Homogeneous Diblocks

In all cases where there was a difference in the effects of adding a heterogeneous versus a homogeneous diblock to s-1,2 PBD and/or trans 1,4 PBD, the effects were more pronounced with the heterogeneous diblocks. These cases are reviewed below.

In blends with 50% or more heterogeneous diblock, the s-1,2 PBD melting point was depressed by 4°-5°C, but in the presence of homogeneous diblock, no significant melting point depression was observed at all.

The mechanical effects of low diblock content discussed in the Section VA are all more pronounced with the 30k/50k and 60k/120k heterogeneous diblocks than with the 30k/200k homogeneous diblock. Tensile modulus dropped more sharply with heterogeneous diblock than with homogeneous diblock. A peak in percent elongation and stress at break occurred in more blends with heterogeneous 30k/50k diblock than with homogeneous 30k/200k diblock. For blends with a t/s ratio of 1/2, addition of heterogeneous diblock led to greater enhancement of mechanical properties at break than did addition of homogeneous diblock. Finally, the crystallinity of the trans 1,4 PBD component increased to a minor degree with the presence of heterogeneous diblock but decreased slightly with the presence of homogeneous diblock.

The two heterogeneous diblocks we studied have different block molecular weights as well as different ratios of block MWs, yet their impact on blends was very similar.

VC. Discussion and Proposed Morphologies

In Section IA, we discussed the relationship between molecular weight and a diblock's ability to compatibilize blends of two homopolymers. A summary of the most evident relationships is as follows: Homopolymers may be solubilized into diblock copolymer domains if the homopolymer MW's are less than the block MWs, especially when the homopolymer content is relatively low. When the block MW's are not equal, the homopolymer

corresponding to the longer block is preferentially solubilized. Alternatively, diblocks may be solubilized into homopolymer domains if the diblock MWs are less than the corresponding homopolymer MW and if the diblock content is low.

Our blends of crystallizable PBD homopolymers plus amorphous PBD diblock copolymer are described better by the second category than by the first: The MWs of the blocks are less than or approximately equal to the MWs of the corresponding homopolymers, and blend properties are enhanced when diblock content is $\leq 10\%$. The MW's of the two blocks in any of the diblocks we studied are not equal, and the block corresponding to the larger MW homopolymer seemed to interact preferentially with that homopolymer. Specifically, we concluded at the end of Section VA that there is a positive interaction between the 1,4 PBD blocks ($MW \leq 200k$ g/mol) and trans 1,4 PBD homopolymer ($MW = 425k$ g/mol) but no apparent interaction between the 1,2 PBD blocks ($MW = 30k-60k$ g/mol) and s-1,2 PBD homopolymer ($MW = 30k$ g/mol). We might have observed more interaction between the 1,2 PBD components if the 1,2 PBD block MWs had been smaller than the MW of the s-1,2 PBD homopolymer.

In general, melting points and crystallinities of s-1,2 PBD and trans 1,4 PBD components in blends with diblock copolymer were not significantly lower than the melting points and crystallinities of the homopolymers. Thus diblock did not penetrate into the crystalline regions of either homopolymer component. Also, recall that all of the blends we tested were heterogeneous, except perhaps blends of only trans 1,4 PBD plus diblock. With these points in mind, morphologies for three categories of blends are proposed below. The categories are as follows: s-1,2 PBD plus diblock, trans 1,4 PBD plus diblock, and finally s-1,2 PBD plus trans 1,4 PBD plus diblock. For each of the categories, we suggest a morphology for low diblock content and for high diblock content. In some cases, we offer distinct morphologies for addition of heterogeneous versus homogeneous diblock copolymer.

In blends of s-1,2 PBD plus diblock copolymer, no property enhancement was observed at any composition. The diblock thus probably segregates from the homopolymer, leaving pools of diblock in a s-1,2 PBD matrix when diblock is the minor component or pools of s-1,2 PBD in a diblock matrix when diblock is the major component.

As mentioned above, there is some type of interaction between the diblocks and trans 1,4 PBD homopolymer. With addition of homogeneous 30k/200k diblock to trans 1,4 PBD homopolymer, the single T_g peak value scaled linearly between the peak values of the homopolymer and 100% 30k/200k diblock, but there was no property enhancement at any composition. Perhaps, true miscibility occurs between this diblock and amorphous regions of the homopolymer. With addition of heterogeneous 30k/50k diblock on the other hand, the T_g peak corresponding to the 1,2 PBD block is distinct at most of the compositions and the mechanical properties in blends with 10% diblock are augmented. In this case, 1,4 PBD blocks may be mixing with amorphous regions of the homopolymer while 1,2 PBD blocks are excluded and forced to form their own phase, as depicted in Figure 20a. When diblock content is low, 1,2 PBD domains formed by the 1,2 PBD blocks may act as filler material to give a response similar to that mentioned at the end of Section IVC for 1,4 PBD homopolymers blended with small amounts of 1,2 PBD.

Finally, in ternary blends of both s-1,2 PBD and trans 1,4 PBD homopolymers plus diblock copolymer, mechanical properties were improved when homogeneous or heterogeneous diblock content was 5%-10%. Enhancement was more pronounced with the heterogeneous diblock copolymer. Also, to achieve property enhancement, we needed slightly more diblock in blends with a trans 1,4 PBD/s-1,2 PBD (t/s) ratio of 2/1 than in blends with t/s=1/2. For example, 10% heterogeneous diblock content gave the best mechanical properties in t/s=2/1 blends, but only 5% heterogeneous diblock content gave the best mechanical results in t/s=1/2 blends. Correspondingly, the interfacial surface area between trans 1,4 PBD and s-1,2 PBD homopolymer domains is greater for t/s=2/1 blends than for t/s=1/2 blends since s-1,2 PBD inclusions are about 0.2μ - 2μ in the former while trans 1,4 PBD inclusions are 0.5μ - 5μ in the latter. These domain sizes were assigned in Section IVC. Interfacial surface area is dependent primarily on the size and distribution of homopolymer domains.

If diblock is located only at this interface in blends with enhanced mechanical properties, then 2%-20% of the interface is covered by diblock. This value is derived in the Appendix. Localization of diblock at the interface accounts for the more advantageous effects of heterogeneous diblock addition over homogeneous diblock addition (Kryszewski, 1980; Shull and Kramer, 1990). With heterogeneous copolymer, micro-phase separated 1,2 PBD blocks

may be forced into s-1,2 PBD homopolymer domains, whereas with homogeneous diblock, the 1,2 PBD blocks are less likely to penetrate into s-1,2 PBD domains - unless heterogeneity is induced in the homogeneous diblock by the presence of homopolymer (Cohen and Torradas, 1984). Figure 20b illustrates ternary blend morphology when diblock is located at the homopolymer interface. In ternary blends with higher than optimal amounts of diblock, the copolymer may form a thick rubber layer at the interface and/or segregate from the homopolymers into its own domains.

Considering that amorphous diblock copolymer did not alter homopolymer crystal structure in any of the blends, our suggested morphologies are not specific for systems with crystallizable homopolymers. They can be applied generally to heterogeneous systems with similar MW relationships, whether or not any of the homopolymer constituents have the ability to crystallize.

VI. General Conclusions

From our work with heterogeneous blends of polybutadienes, we can draw a number of general conclusions regarding the relationship between sample preparation, degree of heterogeneity, and the resulting blend properties, and regarding the role of amorphous diblock copolymer in a blend with two crystallizable homopolymers. The conclusions are listed below:

- 1) Precipitation gives a smaller degree of heterogeneity in blends than do other solvent mixing techniques. The finer dispersion of phases improves mechanical properties. (For systems where properties are poor due to large domains of incompatible materials, precipitation may be successfully exploited to lower the degree of heterogeneity and thereby improve blend properties.)
- 2) Heterogeneous blends of two crystallizable polymers can be advantageously manipulated by addition of amorphous diblock copolymer.
- 3) Furthermore, only a small amount of amorphous diblock is needed to obtain dramatic changes in mechanical properties. (Since amorphous diblock copolymers are easier and less costly to manufacture than diblock copolymers with two crystallizable blocks and since less diblock also means less cost, the commercial implications of our findings are also very important.)

- 4) Heterogeneous diblock copolymers seem to enhance blend properties to a greater extent than homogeneous diblocks.
- 5) In blends with enhanced properties, percent coverage of homopolymer interfacial surface area by diblock is about 2%-20%. Within this range, we can estimate a priori an effective diblock concentration for systems with a known degree of heterogeneity.
- 6) Finally, correlations in the literature regarding MW relationships in blends of homopolymer and diblock copolymer are applicable to our system of crystalline homopolymers plus amorphous diblock copolymer. Specifically, amorphous diblocks can be solubilized by appropriate crystalline homopolymers with MWs greater than the corresponding block, especially when the diblock content is low.

Since homopolymer crystalline structure was not altered by amorphous diblock addition, our conclusions are applicable to heterogeneous systems of amorphous homopolymers as well as crystalline ones.

VII. Potential Areas for Further Study

First, with regard to binary blends of 1,2 PBD and 1,4 PBD homopolymers, the property enhancement in Wilfong's 12/88 amorphous PBD blend and in our 10/90 crystalline PBD blends suggests that 1,2 PBD acts as a reinforcing filler at these low concentrations. PBD blends in this composition range warrant further investigation in future projects, as does the "reinforcing filler" hypothesis.

Second, there are a number of questions that arose during the course of this research that either did not get answered or were not appropriate for our system. Some of the questions relate to binary blends of crystalline homopolymers and some relate to the conditions and extent to which diblock copolymers can emulsify blends of homopolymers, whether or not the homopolymers are crystalline. I list below a sampling of issues that deserve attention with appropriate blend systems and compositions.

Thermodynamic issues: For binary homopolymer blends where the heterogeneous-to-homogeneous transition temperature can be located, can diblock addition - while the homopolymer blend is in the homogeneous state - allow the blend to retain its homogeneity once it reaches temperatures corresponding to the heterogeneous regime? If not, is the resulting degree of

heterogeneity less than if diblock is added while the homopolymer blend is in a heterogeneous state?

Non-equilibrium issues: How does time affect degree of heterogeneity in an amorphous system, and at what point is an equilibrium morphology reached at various temperatures away from the binodal temperature? This question could be investigated with a phase-separated amorphous blend of homopolymers or with a phase-separated crystalline blend in the melt state. What, then, is the effect of diblock copolymer on the development of morphology with time at a given temperature? In addition, other processing and thermal history effects create a range of morphologies worth investigating. For example, we could ask if proven compatibilizers retain their compatibilizing potential when one or more of the blend components are subsequently oriented. Does the orienting process pull the compatibilizer from the interface, and if so what is the effect on the resulting degree of heterogeneity with time?

In our work, we studied binary homopolymer blends where both components crystallized with very fast kinetics. We could also investigate the development of heterogeneity and the role of diblock copolymer in crystalline heterogeneous blends where one component crystallizes at a relatively fast rate and the second component crystallizes at a relatively slow rate.

Finally, in all of the situations suggested above, it is helpful to determine the relative effectiveness of heterogeneous diblocks versus homogeneous diblocks. By investigating these questions, we will greatly add to our understanding of heterogeneous polymer blends and the compatibilization capabilities of diblock copolymers, and thereby increase our ability to control the morphology and properties of blend materials.

References

- Bermudez, S.F., and J.M.G. Fatou, European Polymer Journal, **8**, 575, 1972.
- Billmeyer, Jr., F.W., Textbook of Polymer Science, Third Ed., John Wiley & Sons, 1984.
- Burghardt, W.R., Macromolecules, **22**, 2482, 1989.
- Chow, T.S., Macromolecules, **23**, 333, 1990.
- Cohen, R.E., and J.M. Torradas, Macromolecules, **17**, 1102, 1984.
- Cohen, R.E., and D.E. Wilfong, Macromolecules, **15**, 370, 1982.
- Creton, C., E.J. Kramer, and G. Hadziioannou, Macromolecules, **24**, 1846, 1991.
- deGennes, P.G., Scaling Concepts in Polymer Physics, Cornell University Press, 1979.
- del Giudice, L., R.E. Cohen, G. Attala, and F. Bertinotti, Journal of Applied Polymer Science, **30**, 4305, 1985.
- Drzewinski, M.A., Sc.D. Thesis, Massachusetts Institute of Technology, Cambridge, MA, 1986.
- Elamans, P.H.M., J.M.H. Janssen, and H.E.H. Meijer, Journal of Rheology, **34**(8), 1311, 1990.
- Escala, A., and R.S. Stein, Adv. in Chem. Series, **176**, 455, 1979.
- Flory, P.J., Principles of Polymer Chemistry, Cornell University Press, 1953.
- Hildebrand, J.H. and R.L. Scott, The Solubility of Nonelectrolytes, Dover Publications, 1964.
- Hodge, K.M., G. Kiss, B. Lotz, and J.C. Wittmann, Polymer, **23**, 985, 1982.
- Inoue, T., T. Soen, T. Hashimoto, and H. Kawai, Macromolecules, **3**, 87, 1970.
- Iwayanagi, S., I. Sakurai, T. Sakurai, and T. Seto, Journal of Macromolecular Science - Physics, **B2**, 163, 1968.
- Kinning, D.J., E.L. Thomas, and L.J. Fetters, Macromolecules, **24**, 3893, 1991.
- Kohler, J., G. Riess, and A. Banderet, European Polymer Journal, **4**, 173, 1968.
- Kryszewski, M., Polymer Blends, Proc. Jt. Ital.-Pol. Seminar on Multicomponent Polymer Systems, **1**, 1980.
- Leibler, L. Makromol.Chem., Macromol. Symp., **16**, 1, 1988.

- Leibler, L., H. Orland, and J.C. Wheeler, J. Chem. Phys., **79**, 3550, 1983.
- Manson, J.A., and L.H. Sperling, Polymer Blends and Composites, Plenum Press, 1976.
- McCreehy, K., and H. Keskkula, Polymer, **20**, 1155, 1979.
- Meier, D.J., Polymer Preprints, **18**, 340, 1977.
- Morero, D., F. Ciampelli, and E. Mantica, Advances in Molecular Spectroscopy, Proceedings of the Fourth International Meeting, **2**, 898, A. Mangini, ed., Pergamon Press, England, 1962.
- Morero, D., E. Mantica, and L. Porri, Nuovo Cimento. Suppl., **15**, 10, 136, 1960.
- Natta, G., Science, **147**, 268, 1965.
- Natta, G., G. Allegra, I.W. Gassi, C. Carlino, E. Chiellini, and G. Montognoli, Macromolecules, **2**, 311, 1969.
- Natta G., and P. Corradini, Journal of Polymer Science, **20**, 251, 1956.
- Natta, G., L. Porri, A. Carbonaro, and G. Lugli, Makromolekulare Chemie, **53**, 52, 1962.
- Nishi, T., T. Hayashi, and H. Tanaka, Makromolekulare Chemie, Macromolecular Symposium, **16**, 91, 1988.
- Nishi, T., and T.T. Wang, Macromolecules, **8**(6), 909, 1975.
- Noolandi, J., and K.M. Hong, Macromolecules, **17**, 1531, 1984.
- Olabisi, O., L.M. Robeson, and M.T. Shaw, Polymer-Polymer Miscibility, Academic Press, 1979.
- Paul, D.R., Polymer Blends and Mixtures, D.J. Walsh, J.S. Higgins, and A. Maconnachie, eds., **1**, 1985.
- Paul, D.R., and S. Newman, Polymer Blends, Vol. 1, Academic Press, 1978.
- Ramos, A.R., and R.E. Cohen, Polymer Engineering and Science, **17**, 639, 1977.
- Reiss, G., J. Kohler, C. Tournut, and A. Banderet, Makromolekulare Chemie, **101**, 58, 1967.
- Rim, P.B., and J.P. Runt, Macromolecules, **17**, 1520, 1984.
- Roe, R.J., Macromolecules, **19**, 728, 1986.
- Roe, R., and D. Rigby, Advances in Polymer Science, **82**, 103, 1987.

- Runt, J.P., and P.B. Rim, Macromolecules, 15, 1018, 1982.
- Russell, T.P., H. Ito, and G.D. Wignall, Macromolecules, 21(6), 1703, 1988.
- Scott, R.L., Journal of Chem. Phys., 17, 279, 1949.
- Shull, K.R., and E.J. Kramer, Macromolecules, 23, 4769, 1990.
- Smith, R.W., and J.C. Andries, Rubber Chemistry and Technology, 47, 64, 1974.
- Smith, P., and A.J. Pennings, Polymer, 15, 413, 1974.
- Suzuki, T., H. Tanaka, and T. Nishi, Reports on Progress in Polymer Physics in Japan, 27, 165, 1984.
- Tanaka, H., H. Hasegawa, and T. Hashimoto, Macromolecules, 24, 240, 1991.
- Tanaka, H., A.J. Lovinger, and D.D. Davis, Journal of Polymer Science: Part B: Polymer Physics, 28, 2183, 1990.
- Tanaka, H., and T. Nishi, Physical Review Letters, 55(10), 1102, 1985.
- Tanaka, H., T. Suzuki, and T. Nishi, Reports on Progress in Polymer Physics in Japan, 27, 169, 1984.
- Van Krevelen, D.W., Properties of Polymers: Their Estimation and Correlation with Chemical Structure, Elsevier Scientific Publishing Co., 1976.
- Whitmore, M.D., and J. Noolandi, Macromolecules, 18, 657, 1985.
- Wilfong, D.E., S.M. Thesis, Massachusetts Institute of Technology, Cambridge, MA, 1981.
- Willis, C.L., U.S. Patent #4,480,075, October 30, 1984.
- Wittmann, J.C., and R. St. John Manley, Journal of Polymer Science, Polymer Physics Edition, 15, 1089 and 2277, 1977.
- Xie, H., Y. Liu, M. Jiang, and T. Yu, Makromol. Chem. Rapid Commun., 9, 79, 1988; Polymer, 27, 1928, 1986.

List of Tables and Figures

- Table 1: Thermal Histories and Thermal Properties of Homopolymer Samples
- Table 2: Summary of Homopolymer Characterization Data
- Figure 1: Side-group Placement for Various Tacticities
- Figure 2: General Monomer Units for 1,4 PBD and 1,2 PBD
- Figure 3: Chain Conformations of the Four Stereoisomers of PBD
- Figure 4: Compositions of Blend Samples
- Figure 5: WAXS Scans of Homopolymers
- Figure 6: Crystallization Half-Times as a Function of Undercooling
- Figure 7: Tensile Stress-Strain Data for Precipitated Homopolymers
- Figure 8: Binodal and Spinodal Curves from Flory-Huggins Theory
- Figure 9: Room Temperature WAXS 2θ Scan of 50/50 Blend
- Figure 10: X-ray Scattering Patterns for Homopolymer and 67/33 Blend Melts
- Figure 11: Melting Points of Binary Blends as a Function of Trans 1,4 PBD Content
- Figure 12: Percent Crystallinity as a Function of Trans 1,4 PBD Content
- Figure 13: Binary Blend Tensile Properties as a Function of Trans 1,4 PBD Content (Modulus, Yield Stress, Percent Elongation at Break, Stress at Break)
- Figure 14: Samples that Fractured Along Axis of Tension
- Figure 15: Tensile Modulus a Function of Diblock Content
15a: Blends with 30k/50k Diblock
15b: Blends with 30k/200k Diblock
15c: 1/2 t/s Blends for Three Diblocks
- Figure 16: Yield Stress as a Function of Diblock Content
16a: Blends with 30k/50k Diblock
16b: Blends with 30k/200k Diblock
16c: 1/2 t/s Blends for Three Diblocks
- Figure 17: Percent Elongation at Break as a Function of Diblock Content
17a: Blends with 30k/50k Diblock
17b: Blends with 30k/200k Diblock
17c: 1/2 t/s Blends for Two Heterogeneous Diblocks
17d: 1/2 t/s Blends for One Homogeneous Diblock
- Figure 18: Stress at Break as a Function of Diblock Content
18a: Blends with 30k/50k Diblock
18b: Blends with 30k/200k Diblock
18c: 1/2 t/s Blends for Two Heterogeneous Diblocks
18d: 1/2 t/s Blends for One Homogeneous Diblock
- Figure 19: $\tan \delta$ Curves for Blends with Trans 1,4 PBD plus Diblock
- Figure 20: Proposed Morphologies for Blends with Diblock
20a: Trans 1,4 PBD plus Diblock
20b: Ternary Blends with Diblock at the Homopolymer Interface

Table 1: Thermal Histories and Properties of Homopolymer Samples
(All temperatures in °C)

Sample	History	T_f	T_s	$\%C_f$	$\%C_s$
s-1,2	as-received**		193°		78%
	precip**		189°		74%
	precip		189°		70%
	melt, quench†**		194°		44%
	precip, melt, quench**		188°		46%
	precip, melt, hold* T, quench				
	T= 165°		188°		39%
	T= 155°		187°		38%
	T= 140°		186°		38%
	T= 125°		187°		38%
	T= 110°		186°		39%
	T= 25°		187°		39%
	precip, mold		186°		36%
	precip, mold, melt , cool at 25°		187°		35%
	t- 1,4	as-received**	150°		58%
precip**		134°		54%	
precip		134°		52%	
melt, quench**		141°		41%	
precip, melt, quench**		133°		42%	
precip, melt, hold* T, quench					
T= 165°		133°		44%	
T= 155°		132°		42%	
T= 140°		133°		42%	
T= 125°		133°		41%	
T= 110°		133°		42%	
T= 25°		132°		44%	
precip, mold		137°		52%	
precip, mold, melt , cool at 25°		132°		38%	

Notes:

Error is approximately $\pm 2^\circ\text{C}$ for temperature values and $\pm 4\%$ for %C values.

Where tests were duplicated, average data are presented here.

† All "melted" samples were typically held in the melt in an inert atmosphere for 1-3 minutes.

All quenched samples were cooled from the melt at a rate of -320°C./min.

** No indium standard data were obtained for these samples.

* Isothermally held samples were kept at the hold temperature for 1 minute.

Table 2: Summary of Homopolymer Characterization Data

	Trans 1,4	Syndio 1,2	
	†C-C=C-C†_n	†C-C†_n C C	
MW	425,000 g/mol	32,500 g/mol	(viscometry)
m-struct.	91 +/- 6% 1,4	95 +/- 3% 1,2	(1H NMR)
Tg (os, pk)	-83, -43°C	5, 53°C	(Rheovibron)
Tm	137°C	186°C	(DSC)
Tdeg	245°C	210°C	(DSC)
% crys.	~40%	~50%	(DSC)
crystal	rod-like	spherulitic	(microscopy)
spacing	~1000Å	~200Å	(TEM)

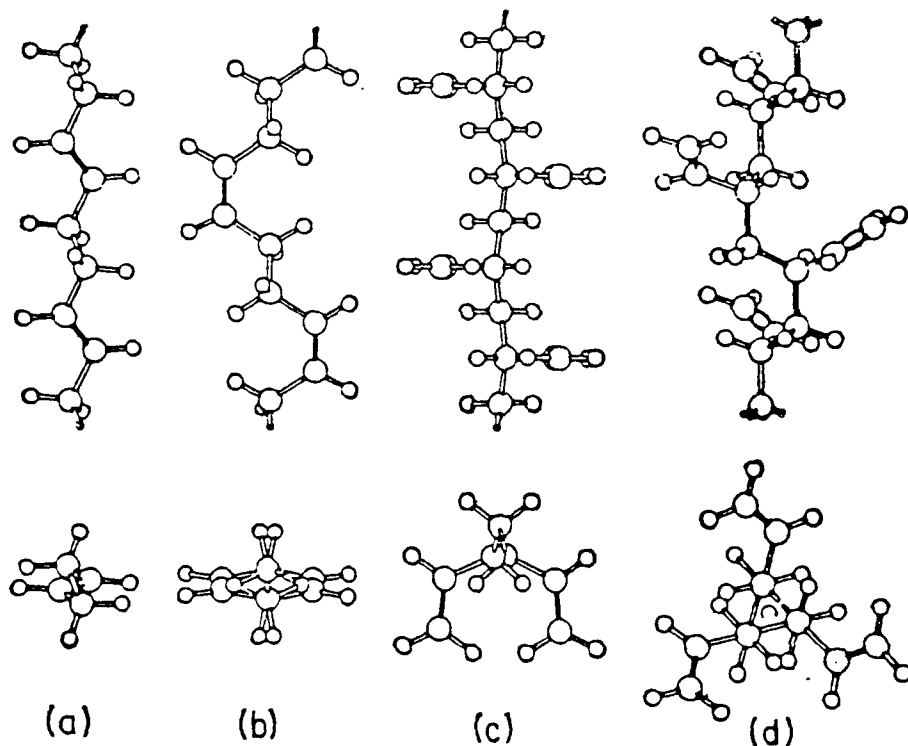
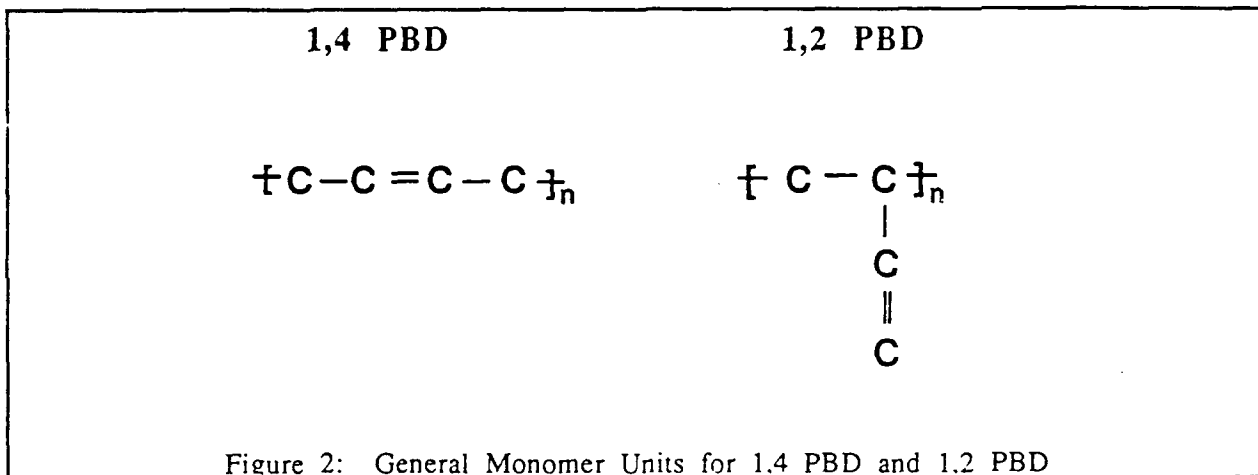
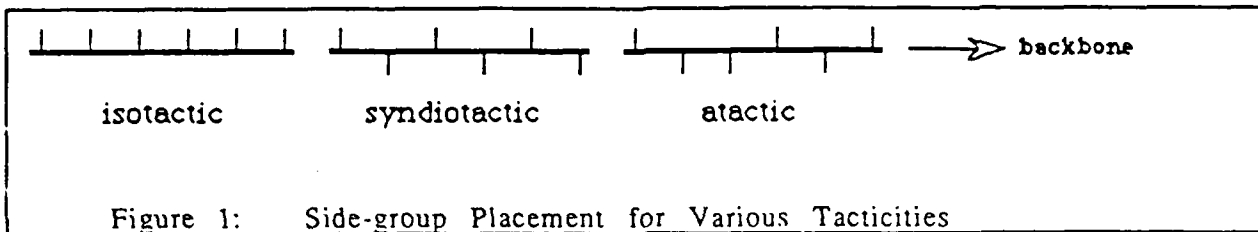


Figure 3. Side and end views of the chain conformations of the four stereoisomers of polybutadiene: (a) *trans*-1,4; (b) *cis*-1,4; (c) syndiotactic-1,2; (d) isotactic-1,2.

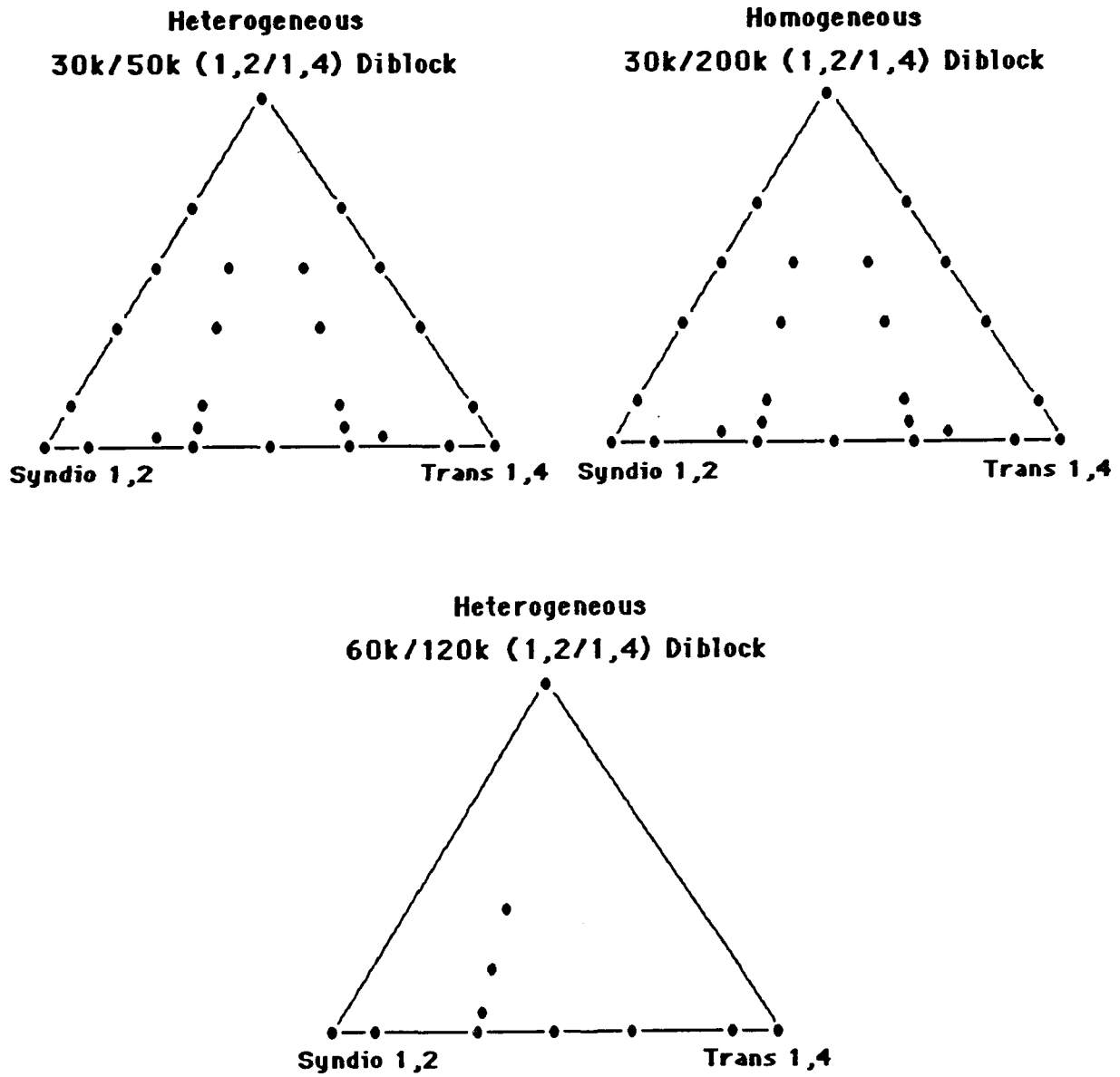
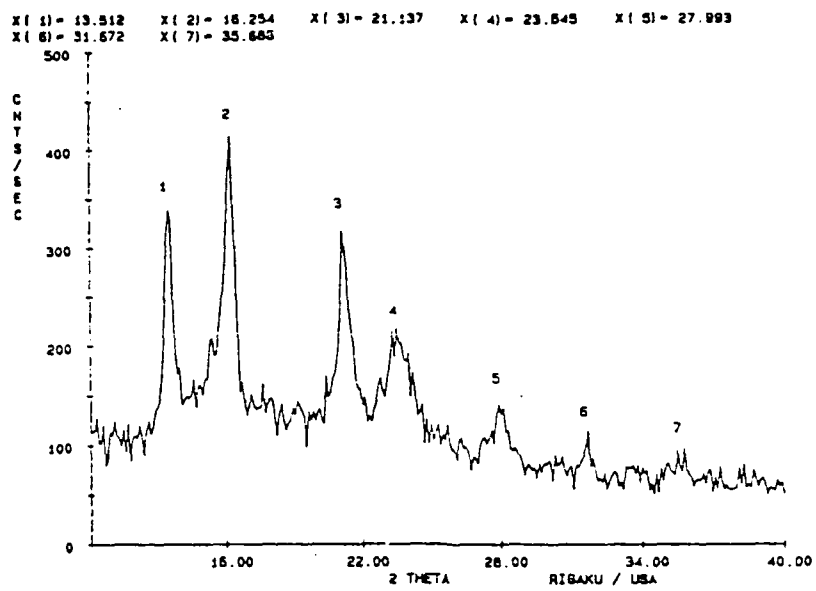
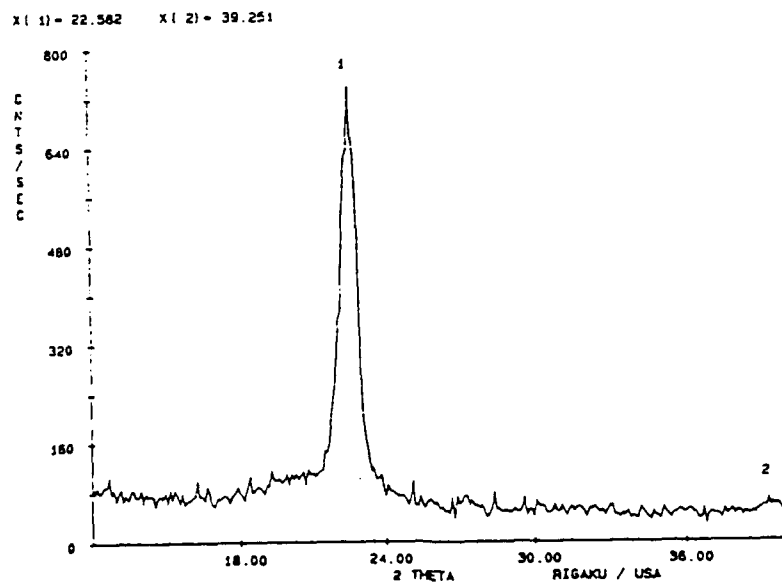


Figure 4: Compositions of Blend Samples



S-1,2 PBD



Trans 1,4 PBD

Figure 5: WAXS Scans of Homopolymers

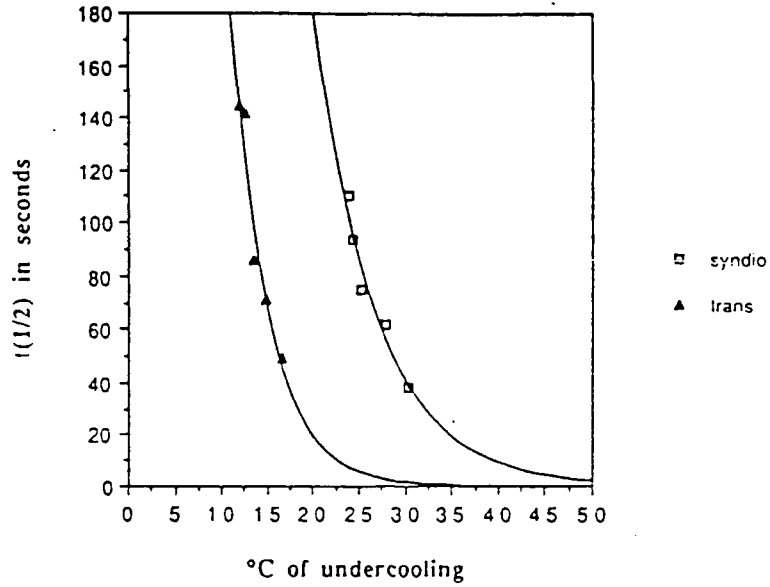
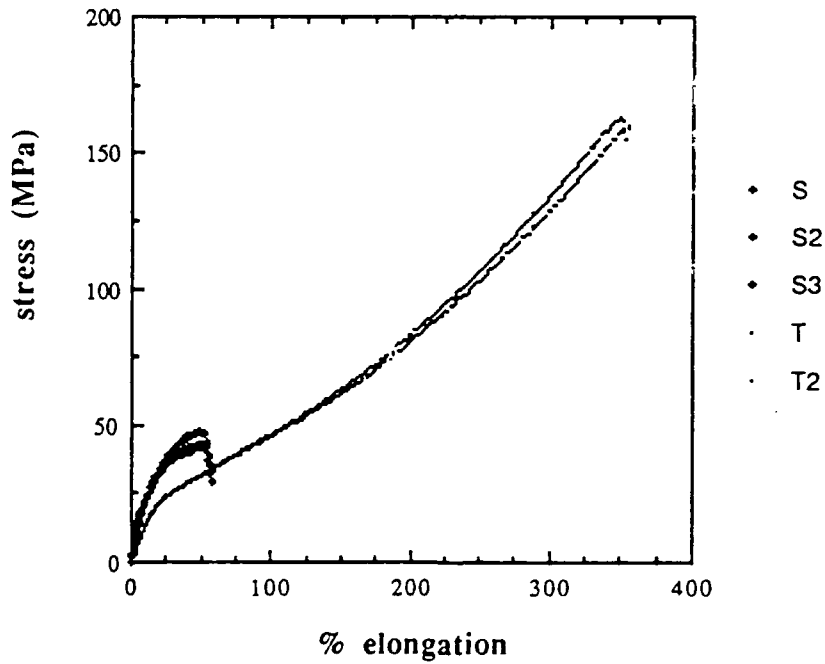


Figure 6: Crystallization Half-Times as a Function of Undercooling

Homopolymer Tensile Tests

(precip, pressed 2 min)



composition	modulus	yd stress	%elng(break)	stress(break)
100/0 (s-1,2)	320 MPa	35 MPa	52%	48 MPa
0/100 (trans 1.4)	140 MPa	22 MPa	354%	163 MPa

Figure 7: Tensile Stress-Strain Data for Precipitated Homopolymers

Binodal and Spinodal with B(avg)

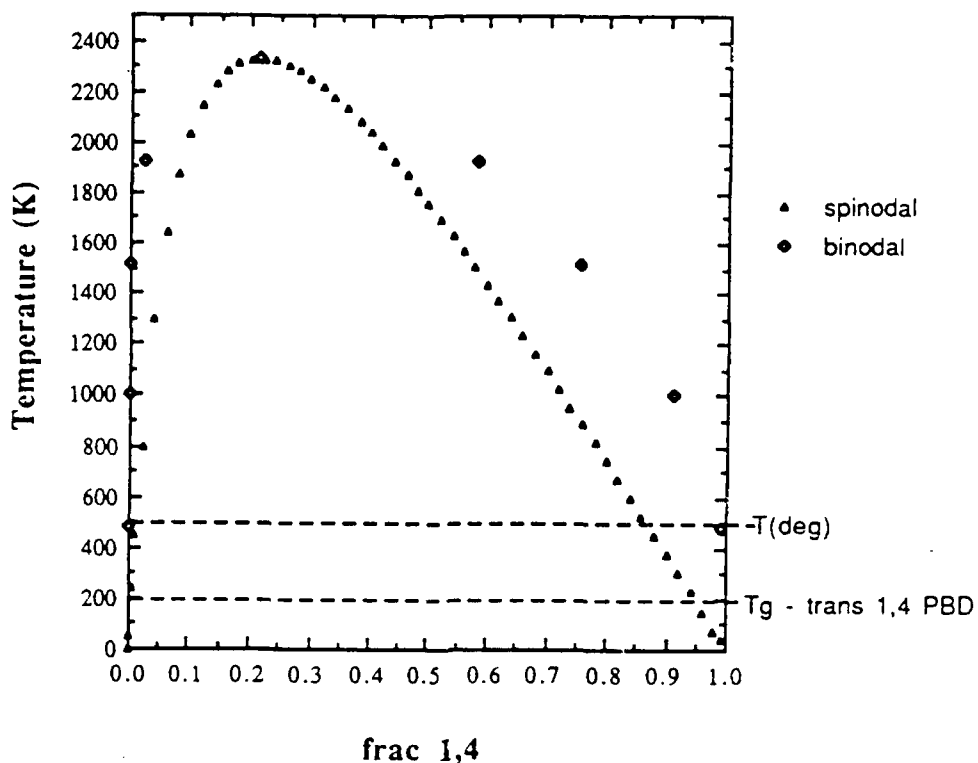


Figure 8: Binodal and Spinodal Curves from Flory-Huggins Theory

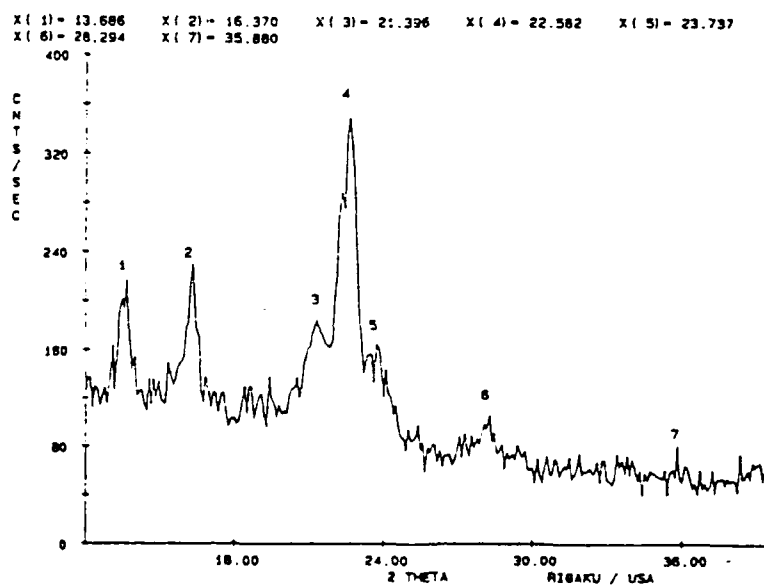


Figure 9: Room Temperature WAXS 2θ Scan of 50/50 Blend

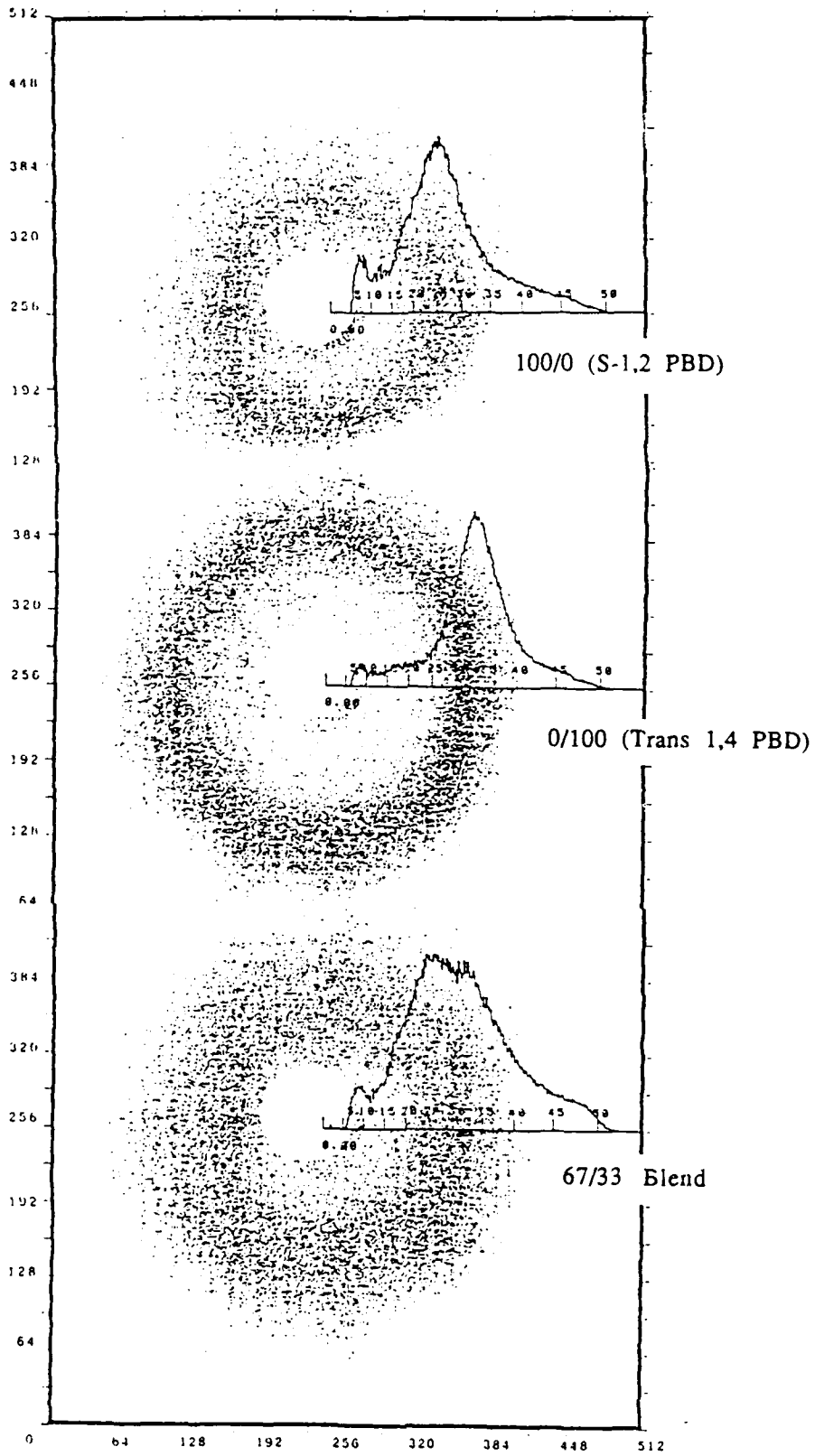


Figure 10: X-ray Scattering Patterns for Homopolymer and 67/33 Blend Melts

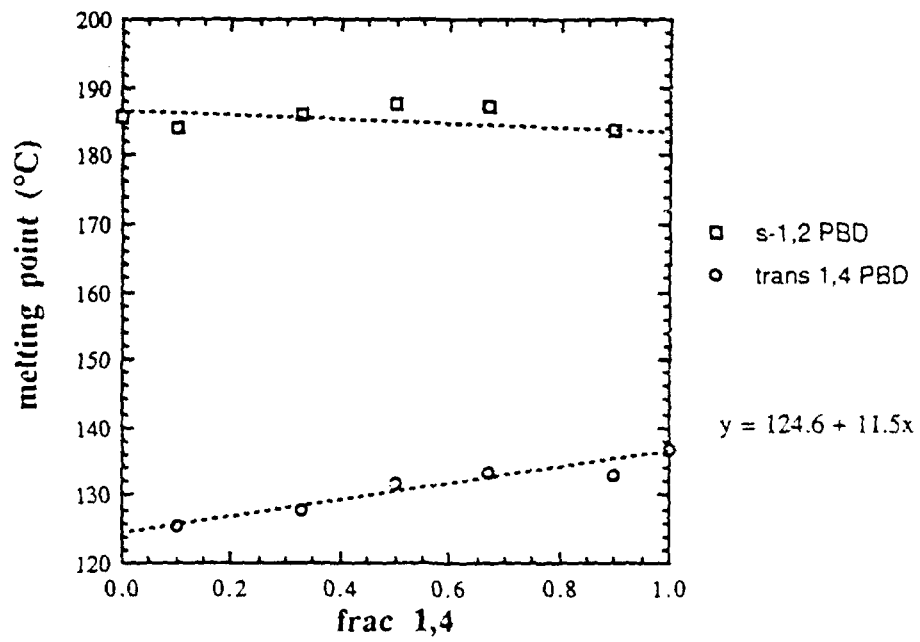


Figure 11: Melting Points of Binary Blends as a Function of Trans 1,4 PBD Content

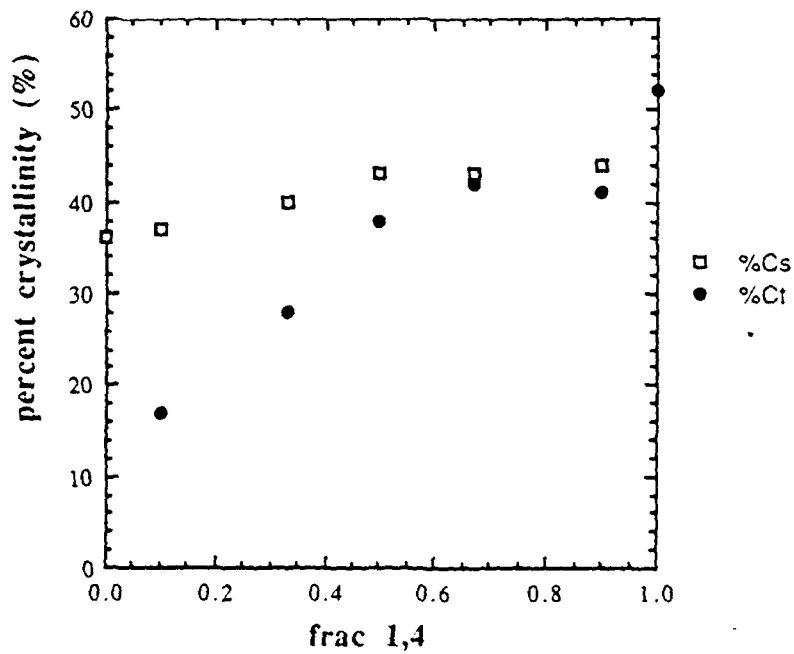


Figure 12: Percent Crystallinity as a Function of Trans 1,4 PBD Content

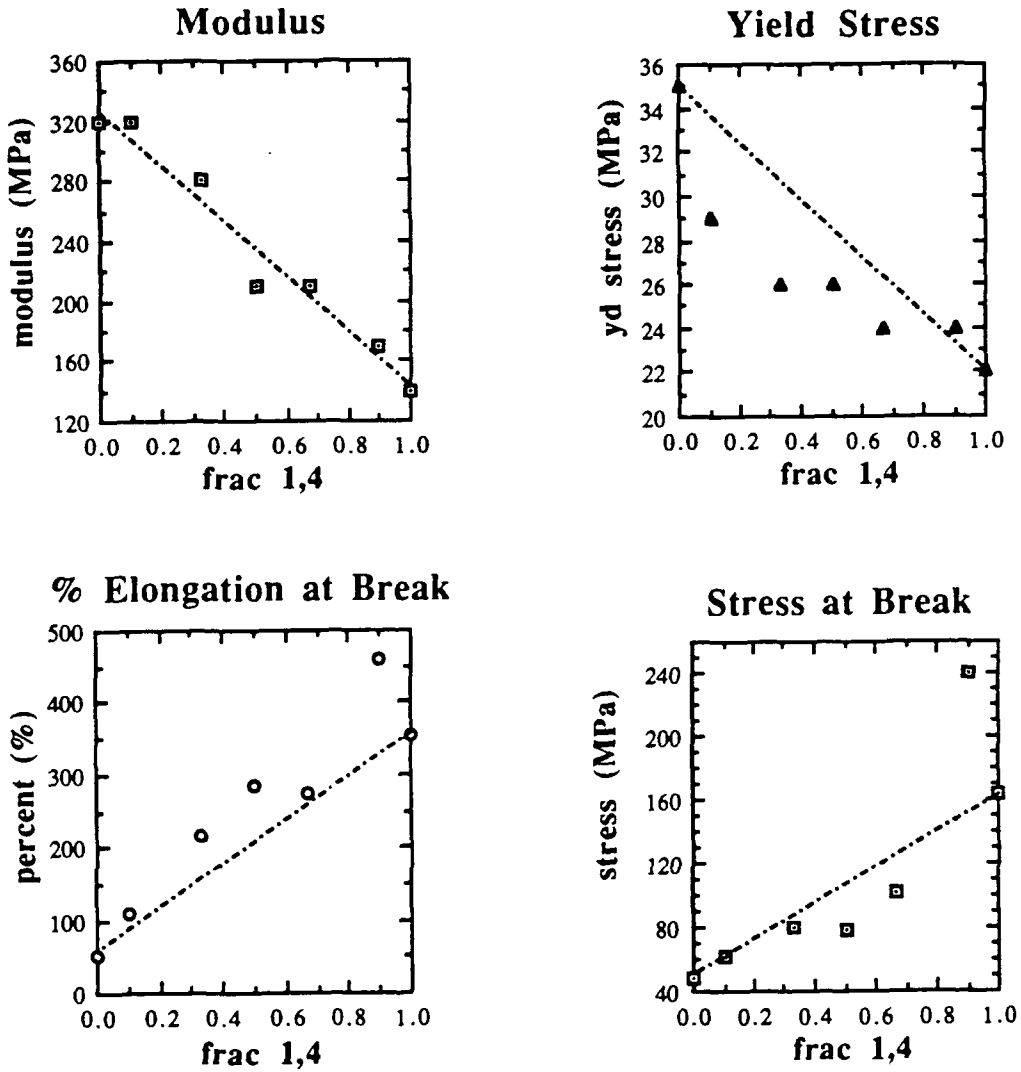


Figure 13: Binary Blend Tensile Properties as a Function of Trans 1,4 PBD Content (Modulus, Yield Stress, Percent Elongation at Break, Stress at Break)

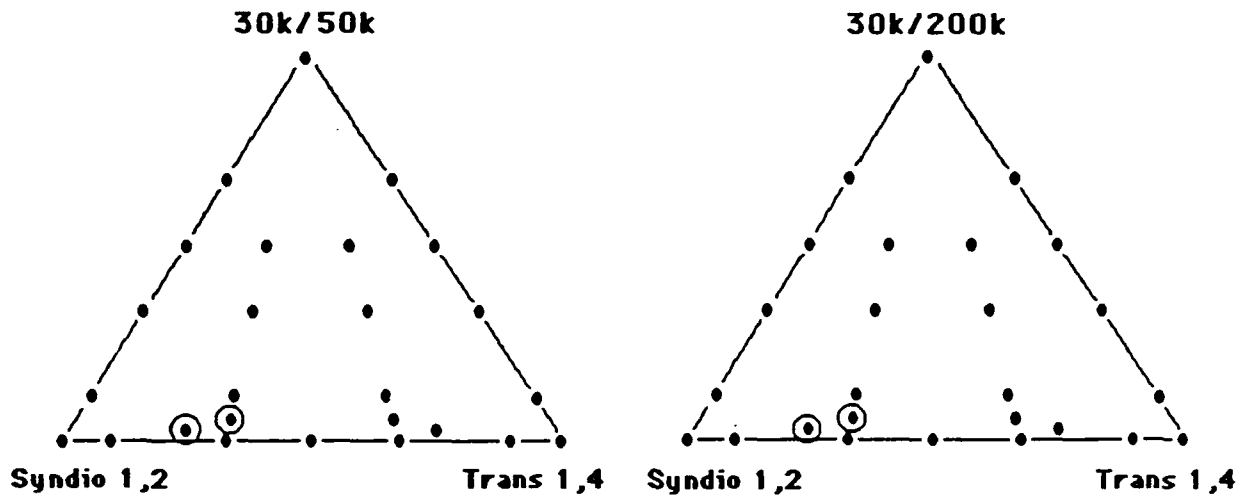
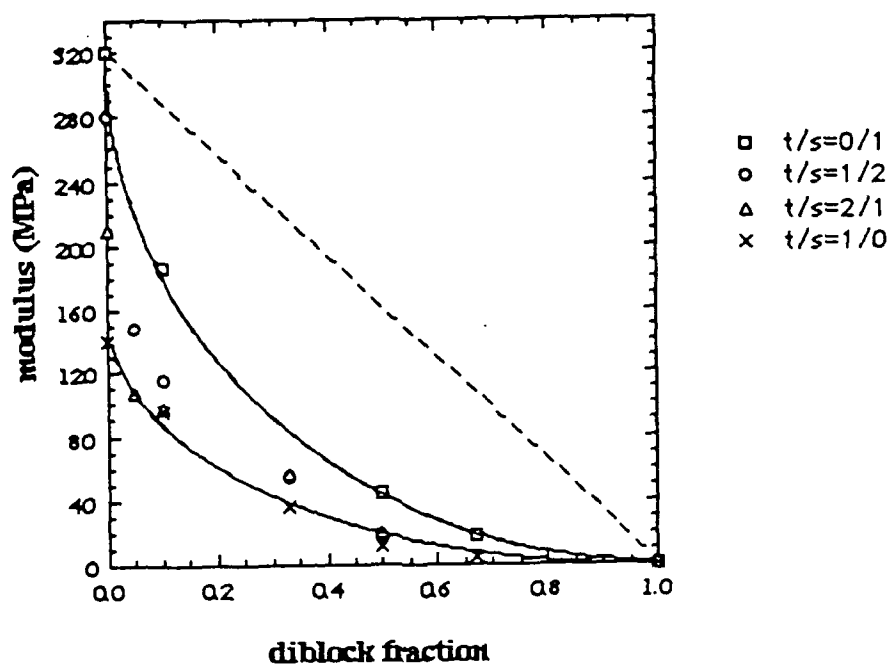


Figure 14: Samples that Fractured Along Axis of Tension
 [74/24/2 and 63/32/5 (s-1,2 PBD/trans 1,4 PBD/ amorphous diblock)]

Moduli of Blends with 30k/50k Diblock



Moduli of Blends with 30k/200k Diblock

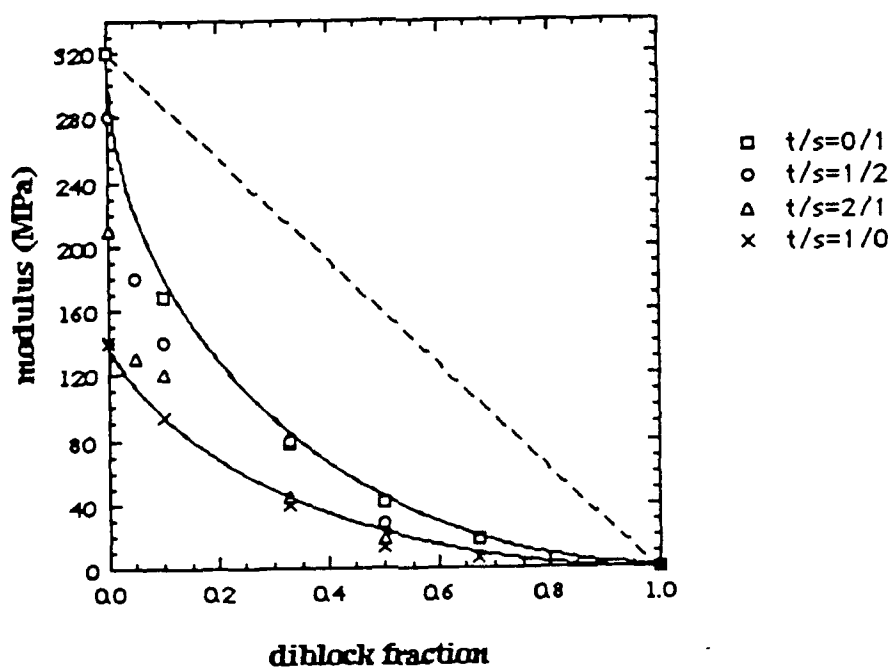
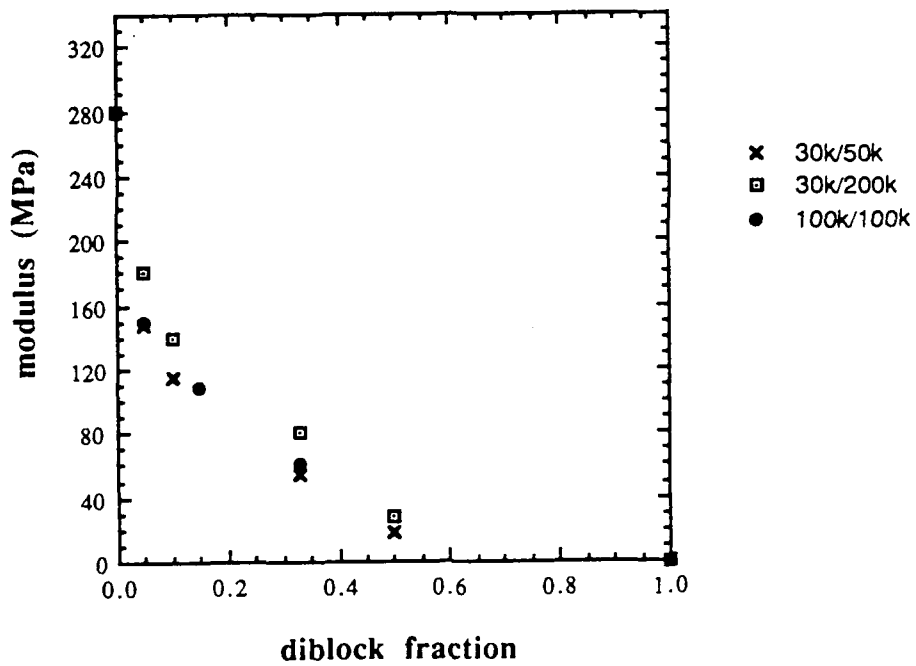


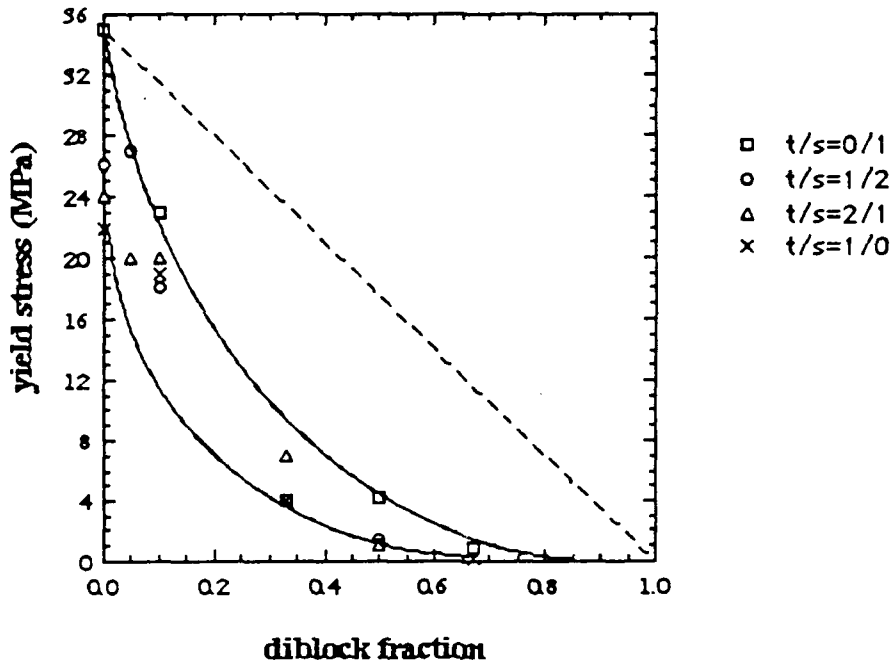
Figure 15: Modulus as a Function of Diblock Content
 15a: Blends with 30k/50k Diblock
 15b: Blends with 30k/200k Diblock

Moduli of 1/2 t/s Blends for Three Diblocks



15c: 1/2 t/s Blends for Three Diblocks

Yield Stress of Blends with 30k/50k Diblock



Yield Stress for Blends with 30k/200k Diblock

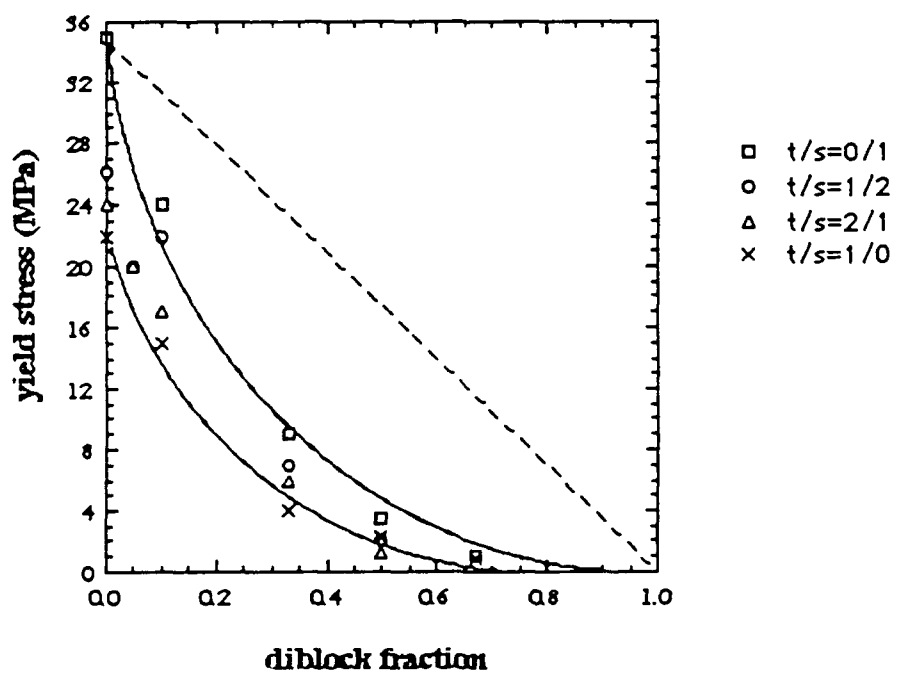
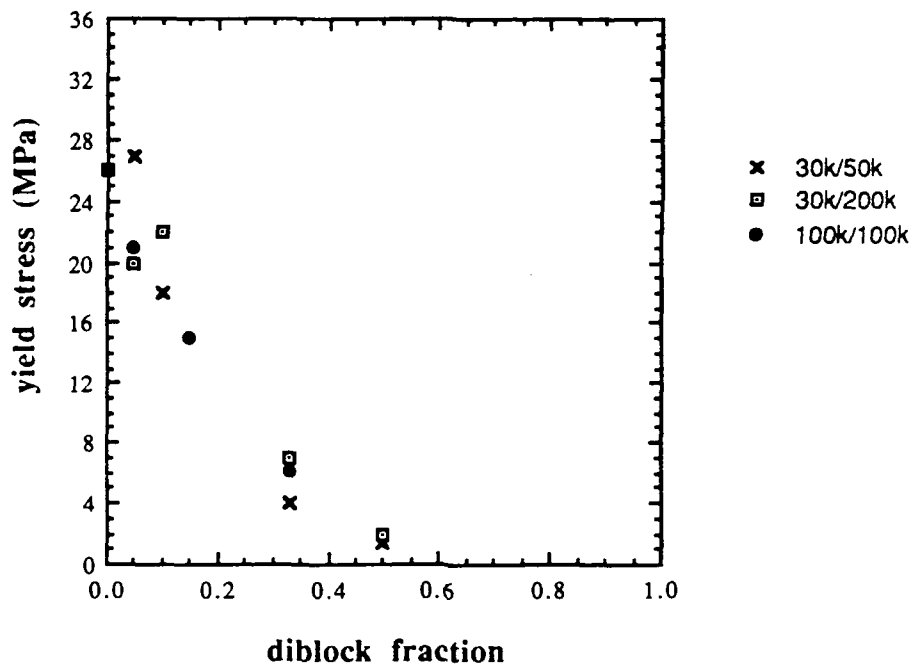


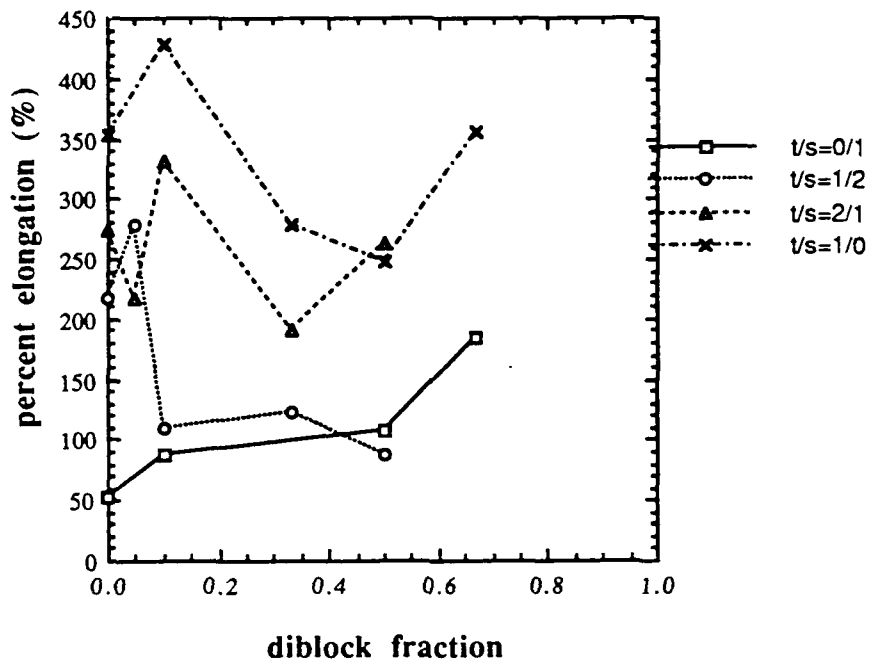
Figure 16: Yield Stress as a Function of Diblock Content
 16a: Blends with 30k/50k Diblock
 16b: Blends with 30k/200k Diblock

Yield Stress of 1/2 t/s Blends with Three Diblocks



16c: 1/2 t/s Blends for Three Diblocks

**% Elongation at Break
for Blends with 30k/50k Diblock**



**% Elongation at Break
for Blends with 30k/200k Diblock**

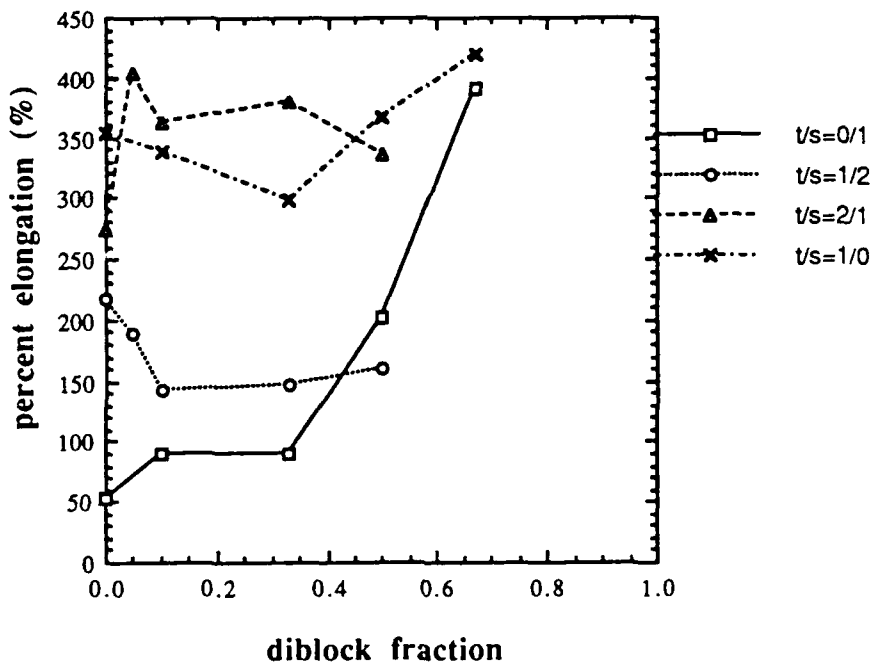
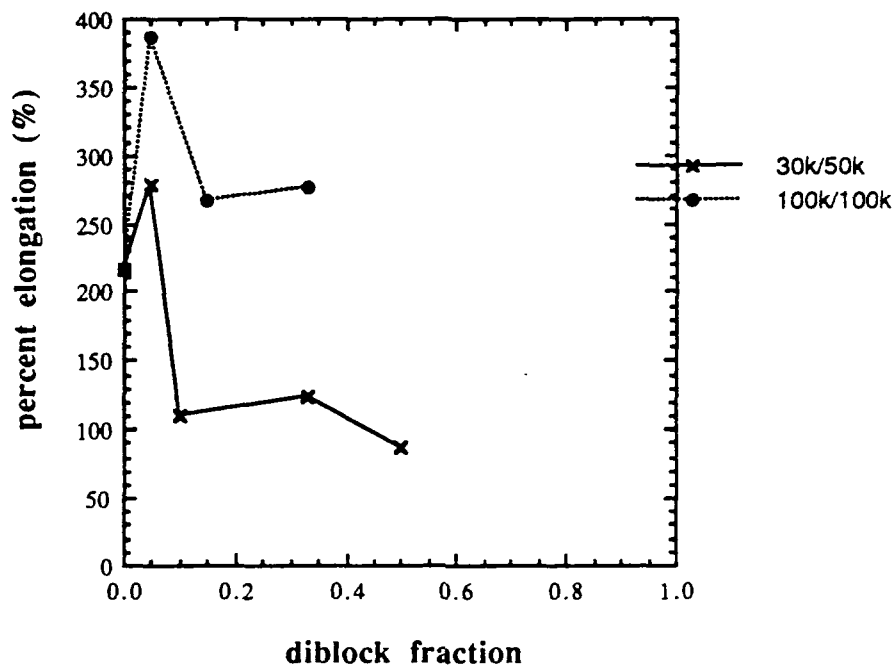
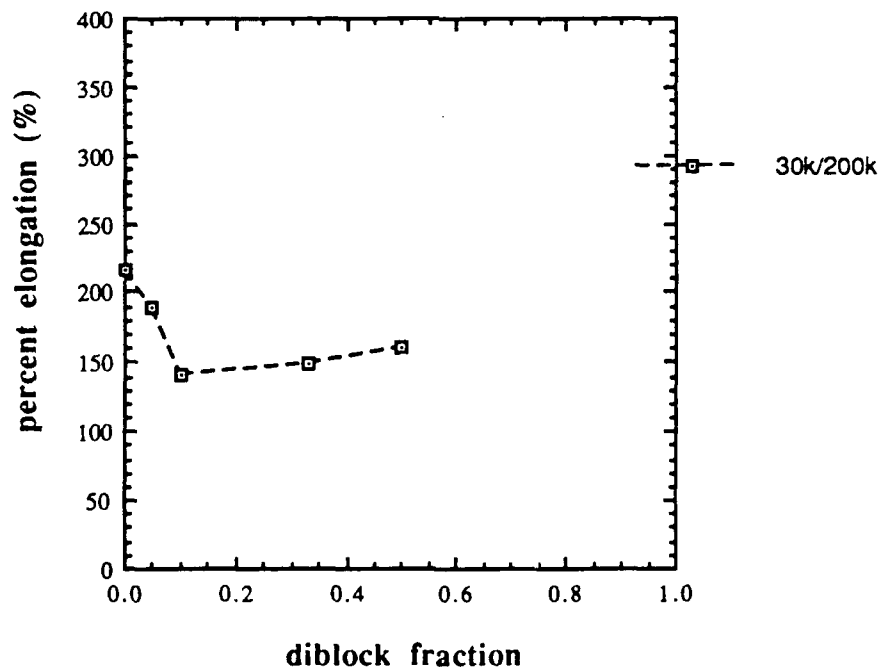


Figure 17: Percent Elongation at Break as a Function of Diblock Content
 17a: Blends with 30k/50k Diblock
 17b: Blends with 30k/200k Diblock

**% Elongation at Break for 1/2 t/s Blends
for Two Heterogeneous Diblocks**

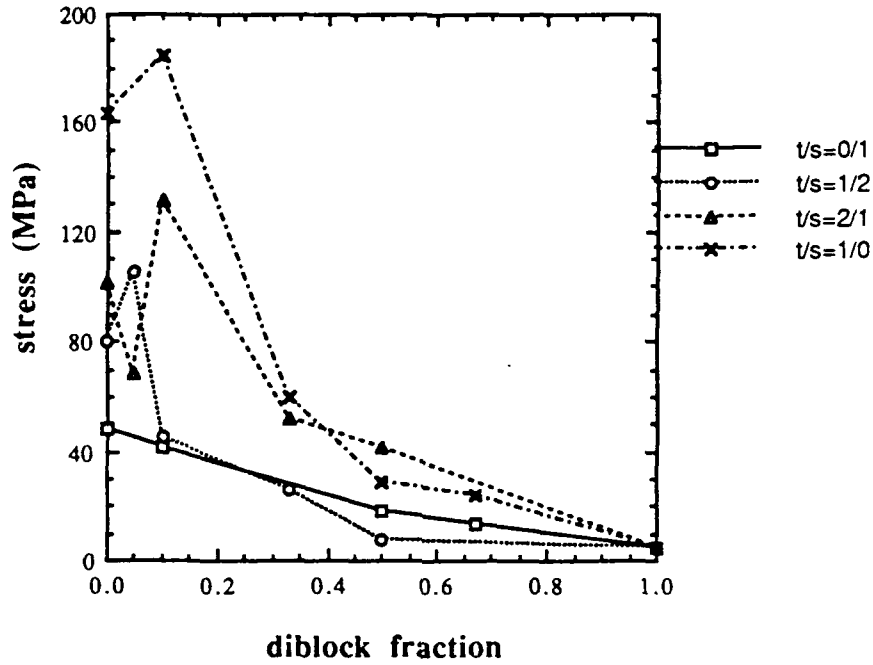


**% Elongation at Break for 1/2 t/s Blends
for One Homogeneous Diblock**



- 17c: 1/2 t/s Blends for Two Heterogeneous Diblocks
 17d: 1/2 t/s Blends for One Homogeneous Diblock

Stress at Break for Blends with 30k/50k Diblock



Stress at Break for Blends with 30k/200k Diblock

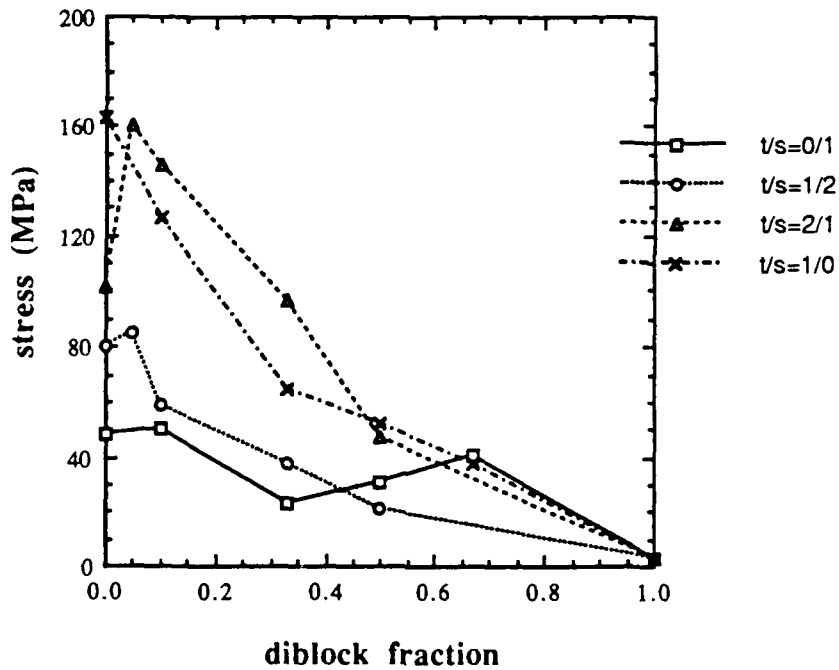
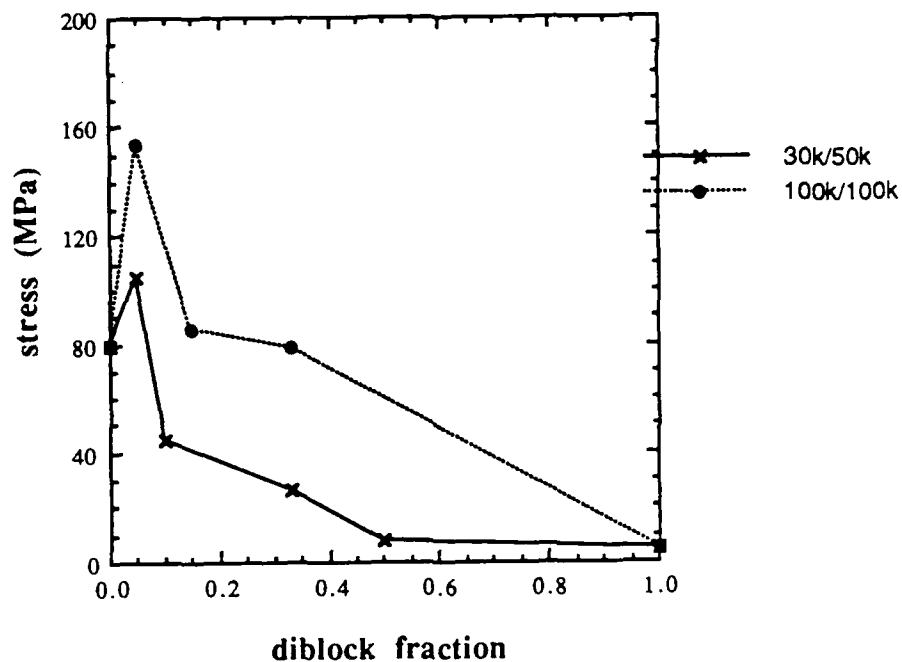
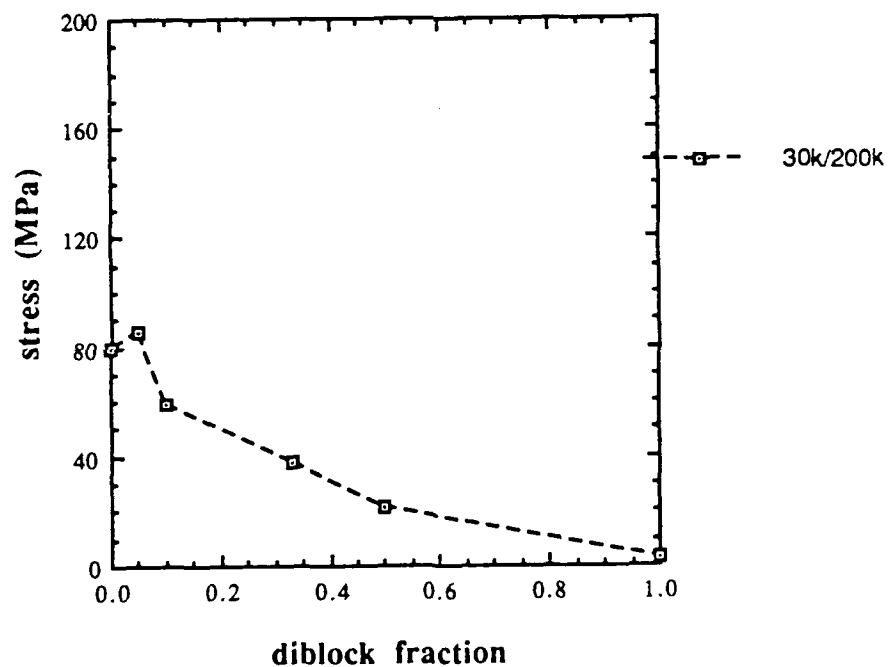


Figure 18: Stress at Break as a Function of Diblock Content
 18a: Blends with 30k/50k Diblock
 18b: Blends with 30k/200k Diblock

**Stress at Break for 1/2 t/s Blends
for Two Heterogeneous Diblocks**

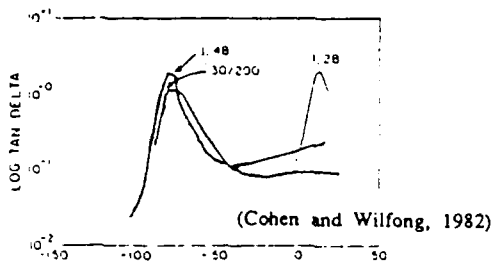


**Stress at Break for 1/2 t/s Blends
for One Homogeneous Diblock**

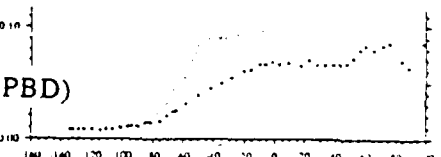
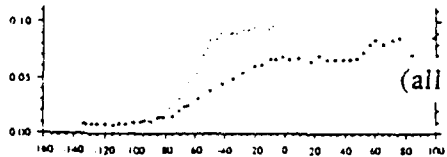
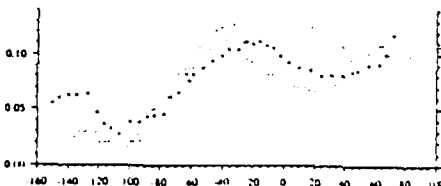
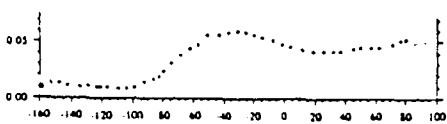
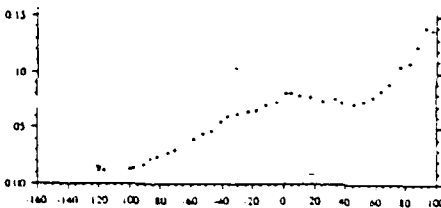
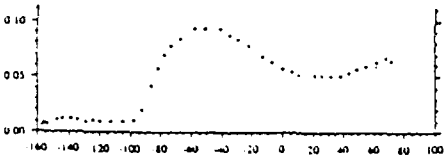
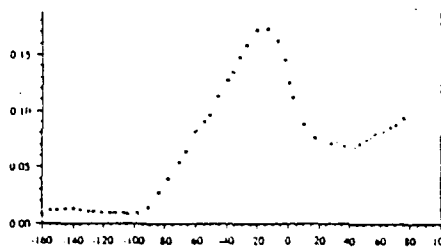
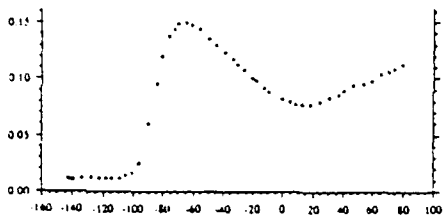
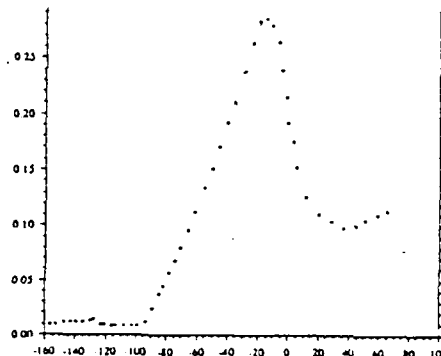
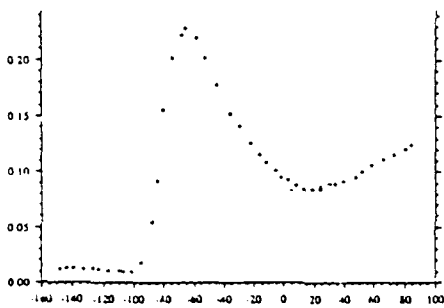
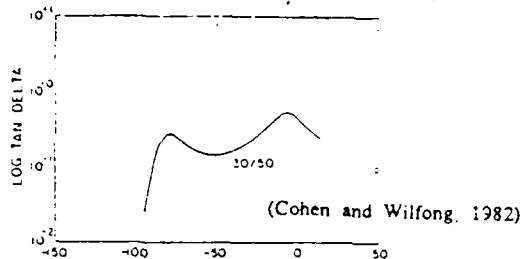


- 18c: 1/2 t/s Blends for Two Heterogeneous Diblocks
- 18d: 1/2 t/s Blends for One Homogeneous Diblock

0/0/100 (all 30k/200k diblock)



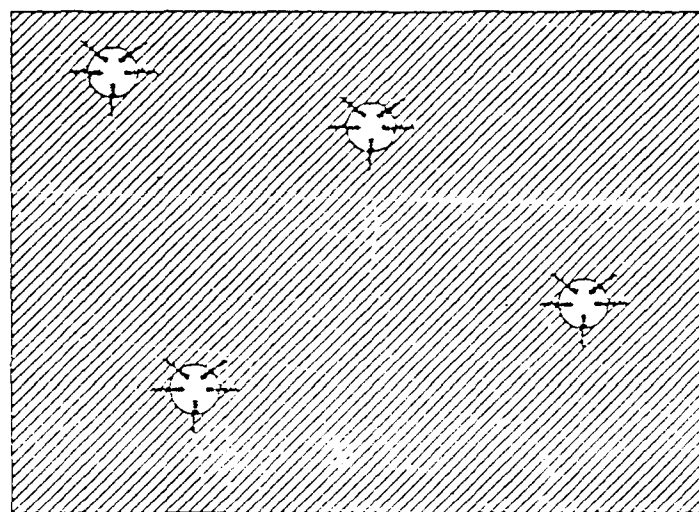
0/0/100 (all 30k/50k diblock)



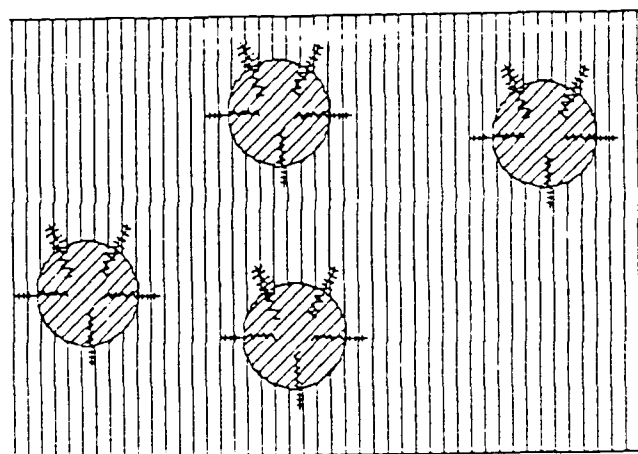
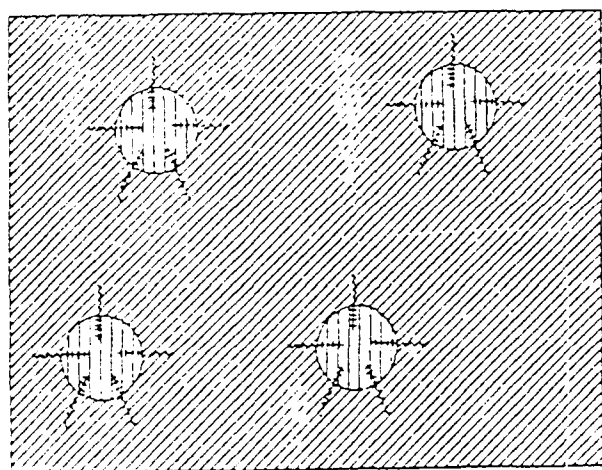
Trans 1,4 PBD plus 30k/200k Diblock

Trans 1,4 PBD plus 30k/50k Diblock

Figure 19: Tan δ Curves for Blends with Trans 1,4 PBD plus Diblock

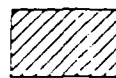


20a.

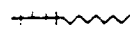


20b.

trans 1,4



s - 1,2



1,2 1,4

Figure 20: Proposed Morphologies for Blends with Diblock
 20a: Trans 1,4 PBD plus Diblock
 20b: Ternary Blends with Diblock at the Homopolymer Interface

Appendix:

PERCENT COVERAGE OF INTERFACIAL SURFACE AREA BY DIBLOCK COPOLYMER

Given Data

1. The peaks in plots of percent elongation at break and stress at break as a function of diblock content occurred at the diblock contents listed below:

<u>t/s ratio in blend</u>	<u>% 30k/50k at peak</u>	<u>% 30k/200k at peak</u>
0/1	-	-
1/2	5% (same w/ 100k/100k)	0-5%
2/1	10%	5%
1/0	10%	-

2. Approximate domain sizes in binary blends of trans 1,4 PBD and s-1,2 PBD are as follows (from Section IVC): Trans 1,4 PBD domains when trans 1,4 PBD is the minor component are $0.5\mu - 5\mu$. S-1,2 PBD domains when s-1,2 PBD is the minor component are $0.2\mu - 2\mu$.

Calculations (based on 1g of polymer total in sample)

1. Total interfacial surface area in t/s = 1/2 and t/s = 2/1 blends:

Assume that domain sizes do not change significantly as diblock is added to system and that domains are spherical in shape.

If [N] = number of spheres of minor component in blend
= (total volume of minor component)/(volume per sphere)
= $V_m/(\pi d_s^3/6)$, where d_s is the diameter of the sphere.

and [SAs] = surface area per sphere
= πd_s^2

then, SA_{total} = total interfacial surface area
= [N] [SAs]
= $[V/(\pi d_s^3/6)] [\pi d_s^2]$
= $6V_m/d_s$

For example, in t/s = 1/2 blends, trans 1,4 PBD is the minor component. With a 1g total polymer basis, $V_m = 0.33g$. Values for "d_s" range from $0.5\mu - 5\mu$ for trans 1,4 PBD, so we get

$$SA_{total} \text{ upper bound} = 40,000 \text{ cm}^2, \quad SA_{total} \text{ lower bound} = 4,000 \text{ cm}^2$$

Similarly, in $t/s = 2/1$ blends, s-1,2 PBD is the minor component. $V_m = 0.33g$ and " d_s " ranges from $0.2\mu - 2\mu$, so

$$SA_{total} \text{ upper bound} = 100,000 \text{ cm}^2, SA_{total} \text{ lower bound} = 10,000 \text{ cm}^2$$

2. Surface Area of Diblock Copolymer at Interface:

The d-spacing, d_d , of one diblock molecule must be on the order of the d-spacings of amorphous 1,4 PBD and 1,2 PBD homopolymers. Based on WAXS data that we obtained for such homopolymers, d_d is about $5.5 \pm 1.0 \text{ \AA}$. Assuming that the diblock aligns at the homopolymer domain interface uncoiled and perpendicular to the plane of the surface, the surface area per diblock molecule at the interface is approximately d_d^2 , or $30 \pm 10 \text{ \AA}^2$. [For reference, Siegmann (1979) lists transverse area per chain of polypropylene and polybutene as 35 \AA^2 and 45 \AA^2 .]

For 1g of a blend with 5% diblock content, where the diblock has a total MW of 80k g/mol to 230k g/mol (as is the case for the 30k/50k and 30k/200k diblocks, respectively), we have

$$(0.05g/MW)(6 \times 10^{23} \text{ molecules/mole}) = 2.5 \pm 1.5 \times 10^{17} \text{ molecules of diblock.}$$

For 10% diblock content, we have $5.0 \pm 3.0 \times 10^{17}$ molecules of diblock.

Thus SA_d = surface area covered by diblock

$$\begin{aligned} &= (30 \text{ \AA}^2/\text{molecule})(\text{number of molecules for given blend}) \\ &= 750 \text{ cm}^2 \text{ for 5\% diblock blends, and} \\ &= 1,500 \text{ cm}^2 \text{ for 10\% diblock blends.} \end{aligned}$$

The error associated with this calculation is on the order of 60% due to the range of diblock MWs.

3. Percent Coverage of Total Interfacial Surface Area by Diblock

We calculated above that blends with $t/s = 1/2$ have SA_{total} values of $40,000 \text{ cm}^2$ to $4,000 \text{ cm}^2$ for 1g samples. Since 5% diblock gave maximal mechanical properties at break, we expect that only 750 cm^2 can be covered by diblock. Thus, diblock accounts for approximately 2%-20% of the total interfacial surface area in these blends.

Similarly, we can calculate percent coverage in blends with $t/s = 2/1$. Here, SA_{total} is $100,000 \text{ cm}^2$ to $10,000 \text{ cm}^2$ for 1g samples. Ten percent heterogeneous diblock gave maximal mechanical properties at break, which corresponds to $1,500 \text{ cm}^2$ of the interface. Actually, these blends contain 0.9g, not 1.0g, total homopolymer, so actual SA_{total} is about 0.9 times $100,000 \text{ cm}^2$ to

10,000 cm². With these numbers, diblock again accounts for approximately 2%-20% of the total interfacial surface area.